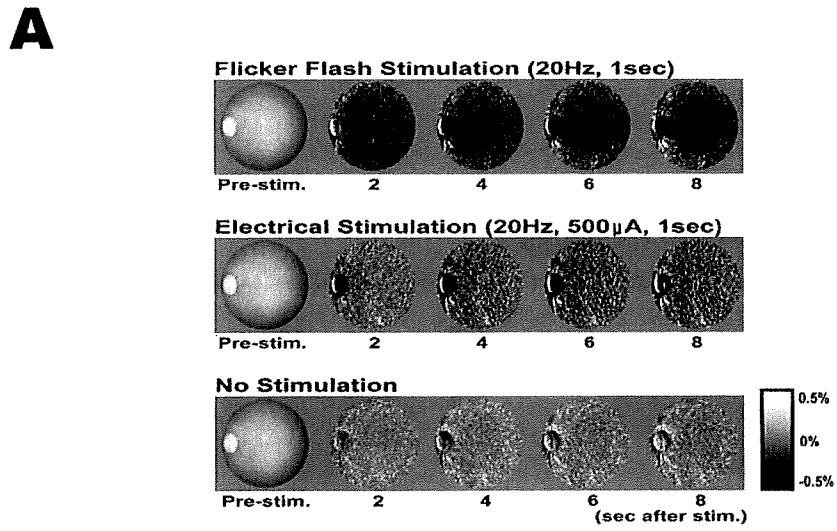

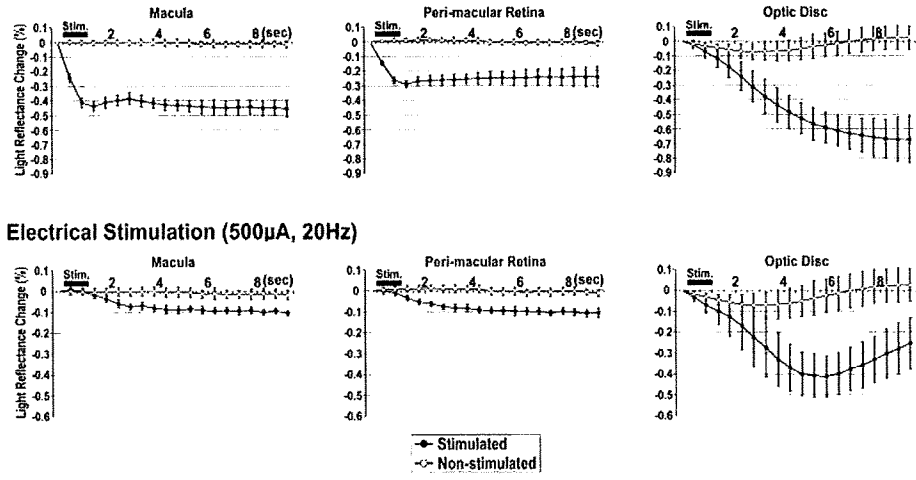

FIGURE 2. Time courses of flash-evoked and electrically evoked intrinsic signals. (A) Monochromatic infrared images of the ocular fundus showing the light reflectance changes during 10 seconds with flicker flash stimulation (*top*) or electrical stimulation (*middle*) or without stimulation (*bottom*). Images on the *left* are fundus images taken before the stimulation. Images on the *right* are the differential images showing the light reflectance changes after stimulation. Thirty consecutive video frames collected during 1 second were averaged for one poststimulus fundus image. Darkened regions indicate a decrease of light reflectance after the light stimulus. The data of three consecutive trials are averaged. (B) Plot of time courses of the light reflectance changes, evoked by flash (*top*) and electrical (*bottom*) stimulation at three different regions in a normal eye. The period of stimulus delivery (1 second) is indicated by *thick bars*. The time after the initiation of stimulus is shown on the abscissa. Data of 10 consecutive trials were averaged.

signals were measured as the stimulus-evoked changes in light reflectance. The amplitude was calculated as poststimulus grayscale values/prestimulus (0.5-second period) values pixel by pixel. This ratio was rescaled to 256 levels of grayscale resolution to show the stimulus-induced reflectance changes (Fig. 2A).

Each recording trial consisted of 300 video frames collected at 30 frames per second for a total recording time of 10 seconds. The grayscale values of 15 video frames collected in 0.5 second were averaged for individual data points to determine the time course of the flash-induced reflectance changes (Fig. 2B).

In our previous studies, we showed that the response properties of the intrinsic signals evoked by a brief light flash were distinctive for different regions of the ocular fundus because they arise from different neuronal and vascular components of the eye, though the precise cellular mechanisms of signal production have not been determined.[25,28] To compare the electrically evoked signals with the light-evoked signals, three retinal regions were examined: the macula (30 × 30 pixels, covering 3.5° of the center), the perimacular region between the macula and the inferior-temporal artery (95 × 25 pixels), and the optic disc (40 × 60 pixels; Fig. 1B). To plot the time courses of reflectance changes, grayscale values within each region were averaged (Fig. 2B).

RESULTS

After flickering light or electrical stimuli, the light reflectance of the posterior retina and the optic disc decreased and the image of the ocular fundus became darker (Fig. 2A, top and middle). The time courses of the intrinsic signals, however, were different for these two stimuli. The time courses of the signals in three regions evoked by light flashes (20 Hz, 1 second, 6.07 cd · s/m^2) and electrical pulses (20 Hz, 1 second, 500 μA) under dark-adapted conditions are shown in Figure 2B. With flickering light, the reflectance changes in the macula and the perimacular retina were more rapid than at the optic disc, with the signal reaching its negative peak within 1.5 seconds after the flash. With electrical stimulation, on the other hand, light reflectance changes in the macula and the perimacular retina were as slow as those at the optic disc. Although the onset of light reflectance changes in the perimacular retina slightly preceded that in the optic disc, the signals in three regions reached their negative peaks 5 to 6 seconds after the stimulus. This trend in the signal time course was the same regardless of the current intensity, for a range of 100 to 1000 μA (data not shown).

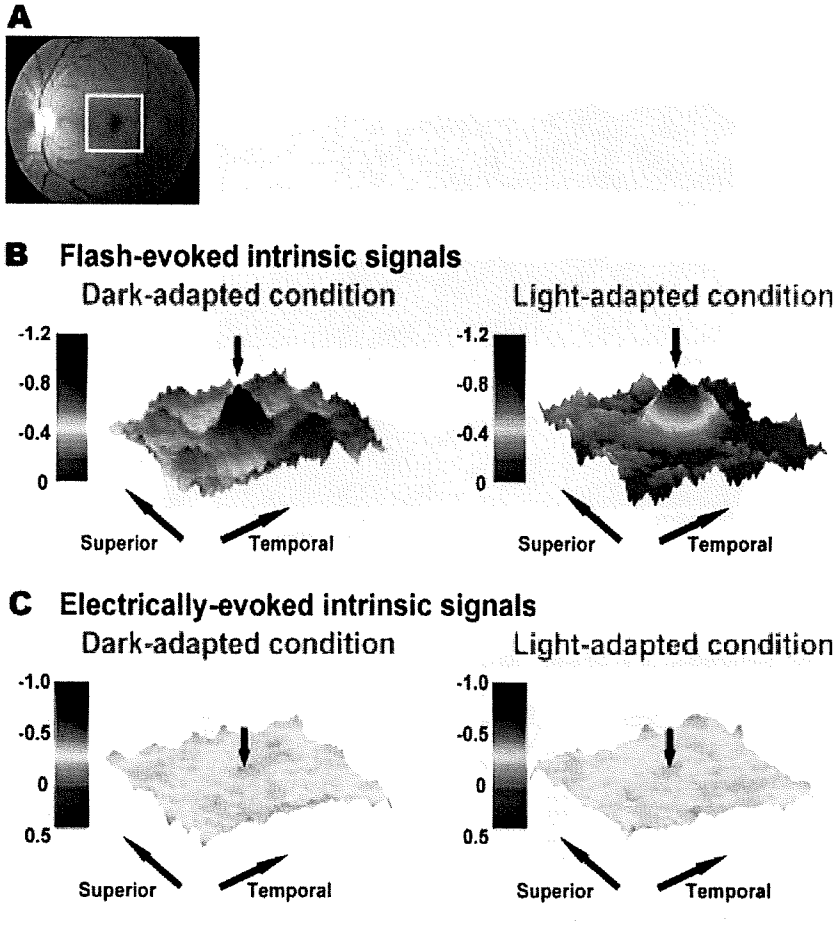

FIGURE 3. Topographic maps of the intrinsic signals elicited by flash-evoked and electrically evoked stimuli in the posterior retina. Pseudocolor topographic maps of light reflectance changes after a single flash (B; flash intensity, 140 cd · s/m^2; duration, 1 msec) or electrical stimulus (C; current, 500 μA; pulse frequency, 20 Hz; stimulus duration, 1 second) in the posterior pole of retina, under dark (*left*)- or light (*right*)-adapted conditions. Twenty consecutive trials were averaged to construct the topographic map. The location of the fovea is indicated by *red arrows*. The region of interest is shown by a *white rectangle* in (A). Note that negative values of light reflectance changes are plotted to indicate the strength of intrinsic signals at each locus.

Spatial Distribution of Intrinsic Signals

Distribution of the intrinsic signals evoked by a flashed light stimulus represents the responses of cone and rod photoreceptors.[25] After 30 minutes of dark adaptation, a topographic map of the intrinsic signal elicited by a flashed light stimulus had a steep peak at the fovea, and the perimacular region was moderately activated (Fig. 3B, left). The strong response at the fovea reflects cone-induced activities, and the response at the perimacular region reflects both cone- and rod-induced activities.[25] In the light-adapted condition, the topography of the response had a steep peak at the fovea, but the response in the perimacular region was strongly reduced because of suppression of rod function (Fig. 3B, right).

The distribution of the electrically evoked signals, on the other hand, did not have a foveal peak in dark- or light-adapted conditions (Fig. 3C). In addition, the perimacular response under dark-adapted conditions did not differ significantly from that under light-adapted conditions. The intrinsic signals evoked by electrical stimulation were roughly homogeneous in the posterior pole, and the spatial distribution did not reflect the anatomic distribution of cone and rod photoreceptors as it did with light stimulation.

Effect of Changes in Stimulus Current

The effect of currents ranging from 0 to 1000 μA on the intrinsic signals was determined under dark- and light-adapted conditions (pulse frequency, 20 Hz; stimulus duration, 1 second; pulse duration, 10 ms; Fig. 4). The peak light reflectance value obtained during the 10-second recording was used for the signal amplitude for each current (same as in Figs. 5 and 6), and the results of three trials were averaged. Results measured at the macula, perimacular retina, and optic disc are shown for two monkeys (M1 and M2). Response properties appear to be approximately the same in each region under both dark- and light-adapted conditions. Change in reflectance as a function of the electrical current was sigmoidal: weak responses were recorded at low currents from 100 to 400 μA, stronger and faster rising signals were recorded above 400 μA, and maximum signals were recorded above 600 μA. The threshold of the electrically evoked intrinsic signals might have been lower than 100 μA in each of the three regions, but it was technically difficult to determine the peak value of the signal when the absolute light reflectance changes became smaller than 0.05%. A small difference of signal amplitudes between dark- and light-adapted conditions in the perimacular area can be noted (Fig. 4, middle graphs); however, this difference was negligible in amplitude and threshold when compared with that in the flash-evoked response, in which twofold to fivefold differences in signal amplitude and a 3-log difference in the threshold of flash intensity were observed between dark- and light-adapted conditions.[28]

Effect of Stimulus Duration

We measured the intrinsic signals evoked by different stimulus durations in the dark-adapted condition. Stimulus durations varied from 0.5, 1, 3, 5, and 7 seconds, pulse frequency was 20 Hz, and stimulus current was 500 μA for a pulse duration of 10 msec (Fig. 5). Results of four trials were averaged in the two monkeys (M1 and M2). Response properties seem to be almost the same in each region; the intrinsic signals increased with longer stimulus durations.

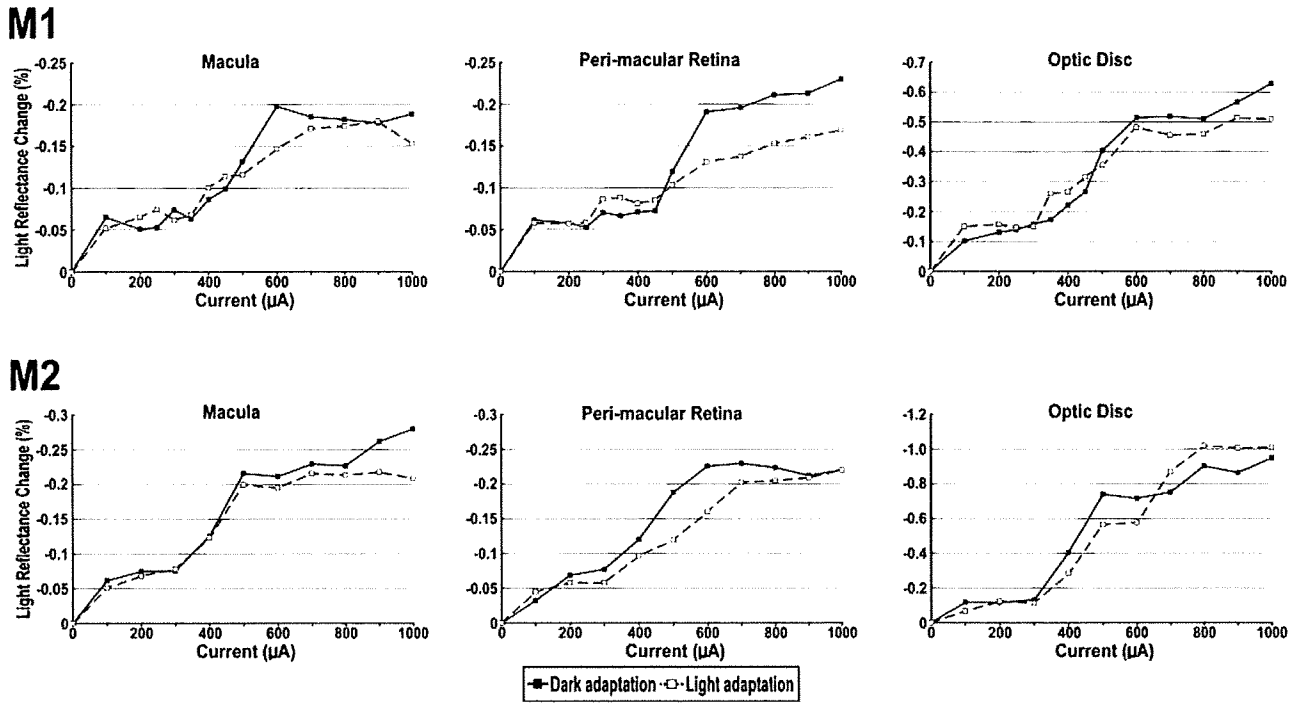

FIGURE 4. Stimulus intensity and intrinsic signals. Changes in the intrinsic signals of three regions after increasing electrical currents (current, 0–1000 μA; total stimulus duration, 1 second; pulse frequency, 20 Hz; pulse duration, 10 msec) in dark- and light-adapted conditions are shown as light reflectance changes in two monkeys (M1 and M2). The peak value of light reflectance decrease during a 10-second recording period was used for the signal amplitude for each current (as in Figs. 5, 6). Note that negative values of light reflectance changes are plotted to indicate the strength of intrinsic signals, and that the vertical scaling is different in three recording regions (as in Figs. 5, 6).

Effect of Stimulus Frequency

We measured the intrinsic signals evoked by different stimulus frequencies under dark-adapted conditions (stimulus current, 500 μA; stimulus duration, 1 second; pulse frequency (Hz)/pulse duration (msec), 5/40, 10/20, 15/13.3, 20/10, 40/5, 60/3.33, 80/2.5, and 100/2; Fig. 6). Results of five trials were averaged for each monkey (M1 and M2).

Response properties seem to have been almost the same in each region; intrinsic signals were maximal when the current frequency was 20 Hz, with one exception in M1 at the peri-macular region (15 Hz). The signal was reduced when the frequency was increased or decreased from 20 Hz.

DISCUSSION

Results of this study showed that electrical stimulation through a DTL electrode resulted in a homogeneous change of light reflectance (intrinsic signals) within the vascular arcades of the retina. Unlike the intrinsic signals induced by light stimuli, a peak of the intrinsic signal was not observed at the fovea, and the threshold of the electrically evoked intrinsic signal was not significantly different for the macula, perimacula, and optic disc. In addition, the threshold did not differ under dark- and light-adapted conditions. The strength of the intrinsic signals increased with longer stimulus durations, and maximum signals were obtained when the stimulus frequency was between 15 and 20 Hz.

There are a number of studies, mainly in vitro experiments using isolated retinas, in which the retinal site activated by electrical stimuli was investigated. Results of most of the studies showed that the site activated—e.g., synaptic terminals of the photoreceptor cells,[29–31] bipolar cells,[32–35] horizontal cells,[36,37] amacrine cells,[38] retinal ganglion cells—was more proximal than the photoreceptors.[14,34,35]

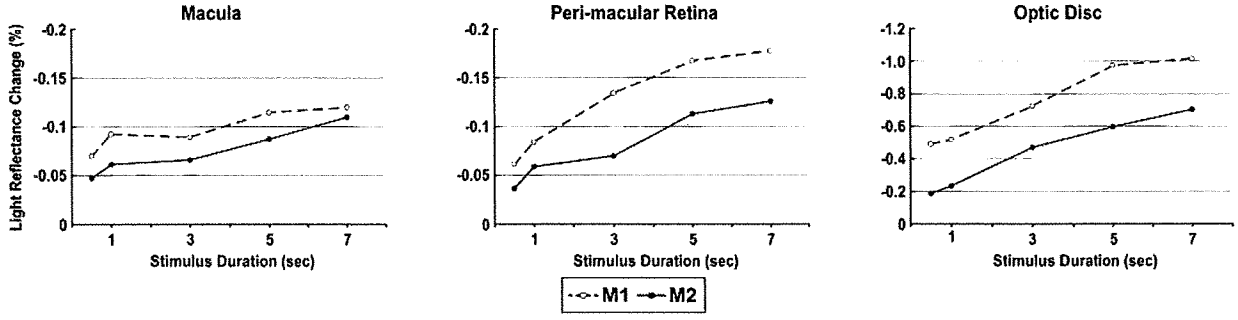

FIGURE 5. Stimulus duration and intrinsic signals. Intrinsic signals of three regions to increasing stimulus durations (total stimulus duration, 0.5 second and 1, 3, 5, and 7 seconds; pulse frequency, 20 Hz; current, 500 μA; pulse duration, 10 msec) in dark-adapted conditions are shown as light reflectance changes for two monkeys (M1 and M2).

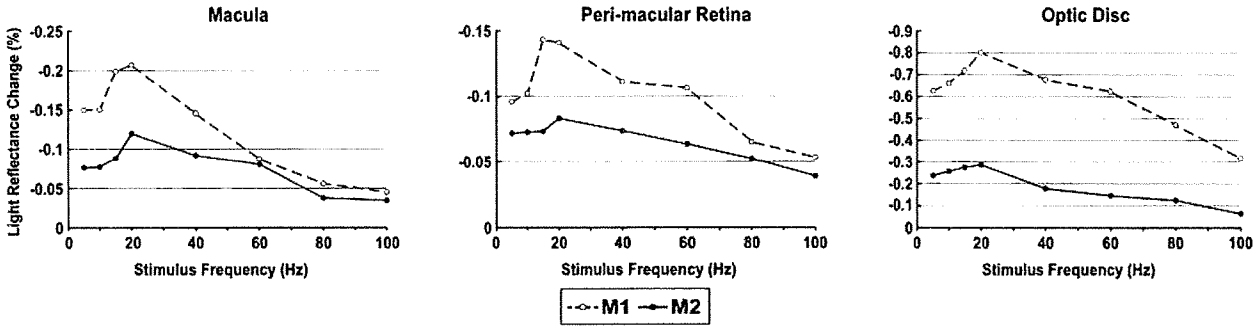

FIGURE 6. Stimulus frequency and intrinsic signals. Intrinsic signals of three regions to increasing stimulus durations (pulse frequency, 5, 10, 15, 20, 40, 60, 80, and 100 Hz; total stimulus duration, 1 second; current, 500 μA) in dark-adapted conditions are shown as light reflectance changes for two monkeys (M1 and M2).

Another method used to identify the site of electrical activation of the retina objectively was the examination of the EER recorded from visual cortex. Thus, Potts et al.[2–4] demonstrated that EER could be recorded in patients with advanced retinitis pigmentosa. They concluded that the site of activation was more central than the photoreceptors.[2–4] Miyake et al.[5–8] showed that the EER is nearly normal in patients with dysfunctional rod or cone visual pathways but that it was extremely abnormal in patients with central artery occlusion. These findings indicate that the retinal origin of EER lies in the middle layer of the retina or close to the retinal ganglion cell layer.[5–8]

The mechanism by which the electrical current is distributed across the retina, however, has not been clearly determined, and the distribution had been estimated mainly by the spatial brightness and extent of phosphenes.[16,39] No study has been reported that estimates the distribution of neural responses over the retina, directly and objectively. In the present study, the current from the DTL electrode enters the eye through the lower anterior part of the sclera and may travel through the vitreous, retina, choroid, or bloodstream to reach the posterior retina. It was not the purpose of this study to investigate the actual pathway of the current. We think a significant amount of the current enters the eye through the sclera and passes through the vitreous body, which also has very low impedance. Brindley[39] designed various types of electrodes that were placed on various locations in the bulbar conjunctiva to investigate the current distribution in the eye by carefully examining the strength and extent of the phosphenes evoked by these electrodes. He concluded that all the electrical phosphenes obtained under the wide range of conditions of his experiments were due to stimulation of the retina by currents flowing perpendicularly to its surface (radial currents through the vitreous humor).[39] Moreover, by observing that the phosphenes were lost as early as 40 seconds from the onset of firm pressure to blind the eye, he concluded that the electrical phosphenes did not result from stimulation of the optic nerve fibers.[39]

When the electrical current is applied from the inferior sclera, one would expect the gradient of stimulation to vary from the inferior retina to the superior retina. Although the current, which spreads radially through the vitreous humor, may not be distributed over the retina in a homogeneous way, the recording region in which quantitative analysis can be reliably conducted is limited to the central 25° in diameter. Thus, we could not measure differences in the signal distribution between the superior and inferior retina outside the vascular arcade.

The retinal intrinsic signals evoked by light stimuli are composed of several components with different properties.[28] Although the precise cellular mechanisms of signal production have not been determined, it is generally believed that the fast signals in the posterior retina (peak time, approximately 150–200 msec) reflect the light-scattering changes after activation of neurons in the outer retina and that the slow signals observed at the posterior retina and the optic disc (peak time, approximately 5–6 seconds) reflect changes in blood flow after neural activation of the cells in the middle or inner layer of the retina. In the later phase, the focally stimulated region showed a focal decrease in light reflectance, with the region corresponding to the location of the stimuli.[28] These findings indicate that the slow components of the intrinsic signals measured in the posterior retina may have a spatial resolution fine enough to indicate the local region of inner retina and can be used for mapping regions made dysfunctional by, for example, glaucoma.

Recently, we showed that the time course of the slow components was strongly correlated with that of blood flow changes measured by laser Doppler flowmetry and that the signals are strongly suppressed by TTX injection into the vitreous cavity, indicating that the slow component of the intrinsic signal are predominantly derived from the stimulus-evoked blood flow increase, which is triggered by the inner retinal activities (Hanazono G, et al. *IOVS* 2007;48:ARVO E-Abstract 528).

In a series of experiments, we have found some discrepancies between the properties of light-evoked and electrically evoked intrinsic signals. First, in the electrically evoked signals, the fast components, which are thought to reflect outer retinal activities, were not observed in the macular and perimacular regions; only slow components were observed (Fig. 2B). Second, the peak of the intrinsic signals in the foveal region evoked by light flashes, which is thought to reflect the activation of foveal cone photoreceptors, could not be observed in the electrically evoked signals, and the response topography in the posterior retina seemed almost homogeneous under dark- and light-adapted conditions (Fig. 3). These findings indicate that the electrical stimuli applied transsclerally do not affect the outer segments of the photoreceptors. We thus believe that the homogenous appearance of the electrically evoked signal may primarily reflect changes induced by the activation of neurons in the inner or middle retinal layers. The most plausible source of the signal is a change in blood flow in the capillaries after activation of the neural cells, although there may be some other cellular mechanisms that can change the light reflectance after electrical stimulation.

When the relationship between the electrical current and the intrinsic signal intensity was examined, we found the response properties seemed to be almost the same under dark- and light-adapted conditions. This is consistent with the previous findings by Miyake,[5] who showed that the amplitude of the EER in humans did not change under dark- and light-adapted conditions. The perceived phosphenes were not altered by the

state of adaptation, and the results of a recent study showed that the threshold of phosphenes is even lower under light-adapted conditions.[16] Taken together with our results, electrical stimulation seems not to be altered by the phototransduction process in the outer segment of photoreceptors.

The relationship between the electrical current and the intrinsic signal intensity was similar in different retinal regions. Under dark- and light-adapted conditions, changes in the intrinsic signal intensity as a function of the electric current were sigmoidal for the three regions studied, and neither the current threshold nor the current giving the maximum intrinsic signal was significantly different. This was, however, not true for the relationship between light intensity and intrinsic signal intensity.[28] In the experiments with light stimuli, the thresholds of intrinsic signals were different, depending on the location of measurement, and the graphs obtained in different regions were completely different. Moreover, there was a shift in threshold to the higher flash intensity to the right after light adaptation. With electrical stimulation, however, the graphs obtained in the three retinal regions were similar and resembled those from the optic disc evoked by light stimulation. This indicates that the electrically evoked intrinsic signals in three regions are related to the blood flow increase after stimulation, though there may be some other mechanisms to induce these signals that are unrelated to blood flow.

With changes in the stimulus frequency of the electrical pulses, the maximal signals were obtained when the current frequency was 20 Hz regardless of the recording region in the ocular fundus. Toi et al.[40] presented an achromatic checkerboard pattern to anesthetized cats and found that the stimulus-related blood flow increase measured by laser Doppler flowmetry was maximum when the stimulus frequency was 20 Hz. The blood flow increase at the optic nerve head after diffuse luminance flicker had physiological properties similar to those of magnocellular retinal ganglion cell neural activities.[41,42] Based on this idea, Riva et al.[43] measured the blood flow increase after 15-Hz flicker stimulus in patients with ocular hypertension and early glaucoma and found that the flicker-evoked blood flow change was abnormally reduced in these patients. These studies suggest a potential in our imaging system to map the dysfunctional regions of the inner retina, such as Bjerrum scotoma in patients with glaucoma. Interestingly, psychophysical studies using flickering stimuli,[44] electrical phosphene,[45] visually evoked potentials,[46] and electrically evoked pupillary reflexes[47] show maximal sensitivities or responses at a frequency of 15 to 20 Hz. The frequency-to-response curves in these studies are similar to those in our study, though the actual sites that regulate this response property are unknown.

In our recording protocol, as the frequency was increased from 5 to 100 Hz, the pulse duration was decreased from 40 to 2 msec, respectively, to keep the total current constant (Fig. 1, inset). There is, however, an in vitro study using isolated salamander retinas, that indicates that the pulse duration is an important factor by which the targeted layer of retina can be determined.[35] The effect of changes in pulse duration in our recording protocol might have influenced the depth of current propagation to some extent.

The resolution of the intrinsic signal topography evoked by electrical stimulation appears to be worse than that evoked by flash stimuli because of the smaller signal amplitudes in the posterior retina. Another factor that might deteriorate the quality of data is the artifacts induced by the electrical current. In a preliminary experiment, we found that currents greater than 1000 μA produce significant artifacts that appear as a mosaic pattern in the posterior pole, possibly because of the muscular contraction of the choroidal arteries by the electrical currents. We found that intrinsic signals could be recorded by transcorneal electrical stimulation by a Burian-Allen contact lens electrode but that the image quality was worse than with transscleral electrical stimulation. This is because the electrical current vibrates the corneal epithelium or the tear film on the cornea, which deteriorates the fundus image observed through the cornea. In our present experimental protocol, we applied the current transsclerally, and it was set lower than 1000 μA to reduce the artifacts.

In conclusion, the results of intrinsic signal imaging indicated that transscleral electrical stimulation is distributed homogeneously over the ocular fundus and represents the activities of neurons mainly in the inner or middle layer of the retina. With further modification of the stimulus protocol and the recording apparatus, it should be possible to record the electrically evoked intrinsic signals in patients. This functional measurement may have potential as a new diagnostic tool for mapping the lesion site of the inner retinal activity, such as Bjerrum scotoma in a patient with glaucoma.

References

1. Motokawa K. Retinal processes and their role in color vision. *J Neurophysiol.* 1949;12:291–303.
2. Potts AM, Inoue J, Buffum D. The electrically evoked response of the visual system (EER). *Invest Ophthalmol.* 1968;7:269–278.
3. Potts AM, Inoue J. The electrically evoked response (EER) of the visual system, II: effect of adaptation and retinitis pigmentosa. *Invest Ophthalmol.* 1969;8:605–612.
4. Potts AM, Inoue J. The electrically evoked response of the visual system (EER), III: further contribution to the origin of the EER. *Invest Ophthalmol.* 1970;9:814–819.
5. Miyake Y, Yanagida K, Yagasaki K. Clinical application of EER (electrically evoked response), I: analysis of EER in normal subjects [in Japanese; author's translation]. *Nippon Ganka Gakkai Zasshi.* 1980;84:354–360.
6. Miyake Y, Yanagida K, Yagasaki K. Clinical application of EER (electrically evoked response), II: analysis of EER in patients with dysfunctional rod or cone visual pathway [in Japanese; author's translation]. *Nippon Ganka Gakkai Zasshi.* 1980;84:502–509.
7. Miyake Y, Yanagida K, Yagasaki K. Clinical application of EER (electrically evoked response), III: analysis of EER in patients with central retinal arterial occlusion [in Japanese; author's translation]. *Nippon Ganka Gakkai Zasshi.* 1980;84:587–593.
8. Miyake Y, Yanagida K, Yagasaki K. Clinical application of EER (electrically evoked response), IV: analysis of EER in patients with optic nerve disease [in Japanese; author's translation]. *Nippon Ganka Gakkai Zasshi.* 1980;84:2047–2052.
9. Miyake Y, Hirose T, Hara A. Electrophysiologic testing of visual functions for vitrectomy candidates, I: results in eyes with known fundus diseases. *Retina.* 1983;3:86–94.
10. Humayun MS, de Juan E Jr, Dagnelie G, Greenberg RJ, Propst RH, Phillips DH. Visual perception elicited by electrical stimulation of retina in blind humans. *Arch Ophthalmol.* 1996;114:40–46.
11. Humayun MS, Weiland JD, Fujii GY, et al. Visual perception in a blind subject with a chronic microelectronic retinal prosthesis. *Vision Res.* 2003;43:2573–2581.
12. Chow AY, Chow VY, Packo KH, Pollack JS, Peyman GA, Schuchard R. The artificial silicon retina microchip for the treatment of vision loss from retinitis pigmentosa. *Arch Ophthalmol.* 2004;122:460–469.
13. Jensen RJ, Ziv OR, Rizzo JF 3rd. Thresholds for activation of rabbit retinal ganglion cells with relatively large, extracellular microelectrodes. *Invest Ophthalmol Vis Sci.* 2005;46:1486–1496.
14. Li L, Hayashida Y, Yagi T. Temporal properties of retinal ganglion cell responses to local transretinal current stimuli in the frog retina. *Vision Res.* 2005;45:263–273.
15. Delbeke J, Pins D, Michaux G, Wanet-Defalque MC, Parrini S, Veraart C. Electrical stimulation of anterior visual pathways in retinitis pigmentosa. *Invest Ophthalmol Vis Sci.* 2001;42:291–297.
16. Gekeler F, Messias A, Ottinger M, Bartz-Schmidt KU, Zrenner E. Phosphenes electrically evoked with DTL electrodes: a study in patients with retinitis pigmentosa, glaucoma, and homonymous

visual field loss and normal subjects. *Invest Ophthalmol Vis Sci.* 2006;47:4966–4974.

17. Morimoto T, Miyoshi T, Matsuda S, Tano Y, Fujikado T, Fukuda Y. Transcorneal electrical stimulation rescues axotomized retinal ganglion cells by activating endogenous retinal IGF-1 system. *Invest Ophthalmol Vis Sci.* 2005;46:2147–2155.
18. Miyake K, Yoshida M, Inoue Y, Hata Y. Neuroprotective effect of transcorneal electrical stimulation on the acute phase of optic nerve injury. *Invest Ophthalmol Vis Sci.* 2007;48:2356–2361.
19. Fujikado T, Morimoto T, Matsushita K, Shimojo H, Okawa Y, Tano Y. Effect of transcorneal electrical stimulation in patients with nonarteritic ischemic optic neuropathy or traumatic optic neuropathy. *Jpn J Ophthalmol.* 2006;50:266–273.
20. Inomata K, Shinoda K, Ohde H, et al. Transcorneal electrical stimulation of retina to treat longstanding retinal artery occlusion. *Graefes Arch Clin Exp Ophthalmol.* 2007;245(12):1773–1780.
21. Grinvald A, Lieke E, Frostig RD, Gilbert CD, Wiesel TN. Functional architecture of cortex revealed by optical imaging of intrinsic signals. *Nature.* 1986;324:361–364.
22. Bonhoeffer T, Grinvald A. Optical imaging based on intrinsic signals: the methodology. In: Toga AW, Mazziotta JC, eds. *Brain Mapping.* San Diego: Academic Press; 1996:55–97.
23. Tsunoda K, Yamane Y, Nishizaki M, Tanifuji M. Complex objects are represented in macaque inferotemporal cortex by the combination of feature columns. *Nat Neurosci.* 2001;4:832–838.
24. Okawa Y, Fujikado T, Miyoshi T, et al. Optical imaging to evaluate retinal activation by electrical currents using suprachoroidal–transretinal stimulation. *Invest Ophthalmol Vis Sci.* 2007;48:4777–4784.
25. Tsunoda K, Oguchi Y, Hanazono G, Tanifuji M. Mapping cone- and rod-induced retinal responsiveness in macaque retina by optical imaging. *Invest Ophthalmol Vis Sci.* 2004;45:3820–3826.
26. Abramoff MD, Kwon YH, Ts'o D, et al. Visual stimulus-induced changes in human near-infrared fundus reflectance. *Invest Ophthalmol Vis Sci.* 2006;47:715–721.
27. Crittin M, Riva CE. Functional imaging of the human papilla and peripapillary region based on flicker-induced reflectance changes. *Neurosci Lett.* 2004;360:141–144.
28. Hanazono G, Tsunoda K, Shinoda K, Tsubota K, Miyake Y, Tanifuji M. Intrinsic signal imaging in macaque retina reveals different types of flash-induced light reflectance changes of different origins. *Invest Ophthalmol Vis Sci.* 2007;48:2903–2912.
29. Crapper DR, Noell WK. Retinal excitation and inhibition from direct electrical stimulation. *J Neurophysiol.* 1963;26:924–947.
30. Knighton RW. An electrically evoked slow potential of the frog's retina, I: properties of response. *J Neurophysiol.* 1975;38:185–197.
31. Stett A, Barth W, Weiss S, Haemmerle H, Zrenner E. Electrical multisite stimulation of the isolated chicken retina. *Vision Res.* 2000;40:1785–1795.
32. Kaneko A, Saito T. Ionic mechanisms underlying the responses of off-center bipolar cells in the carp retina, II: studies on responses evoked by transretinal current stimulation. *J Gen Physiol.* 1983;81:603–612.
33. Toyoda J, Fujimoto M. Application of transretinal current stimulation for the study of bipolar-amacrine transmission. *J Gen Physiol.* 1984;84:915–925.
34. Shimazu K, Miyake Y, Watanabe S. Retinal ganglion cell response properties in the transcorneal electrically evoked response of the visual system. *Vision Res.* 1999;39:2251–2260.
35. Margalit E, Thoreson WB, Inner retinal mechanisms engaged by retinal electrical stimulation. *Invest Ophthalmol Vis Sci.* 2006;47:2606–2612.
36. Byzov AL, Trifonov JA. The response to electric stimulation of horizontal cells in the carp retina. *Vision Res.* 1968;8:817–822.
37. Murakami M, Takahashi K. Calcium action potential and its use for measurement of reversal potentials of horizontal cell responses in carp retina. *J Physiol.* 1987;386:165–180.
38. Takahashi K, Murakami M. Calcium action potential in ON-OFF transient amacrine cell of the carp retina. *Brain Res.* 1988;456:29–37.
39. Brindley GS. The site of electrical excitation of the human eye. *J Physiol.* 1955;127:189–200.
40. Toi VV, Riva CE. Variations of blood flow at optic disc nerve head induced by sinusoidal flicker stimulation in cats. *J Physiol.* 1994;482:189–202.
41. Falsini B, Riva CE, Logean E. Flicker-evoked changes in human optic nerve blood flow: relationship with retinal neural activity. *Invest Ophthalmol Vis Sci.* 2002;43:2309–2316.
42. Riva CE, Logean E, Falsini B. Temporal dynamics and magnitude of the blood flow response at the optic disk in normal subjects during functional retinal flicker-stimulation. *Neurosci Lett.* 2004;356:75–78.
43. Riva CE, Salgarello T, Logean E, Colotto A, Galan EM, Falsini B. Flicker-evoked response measured at the optic disc rim is reduced in ocular hypertension and early glaucoma. *Invest Ophthalmol Vis Sci.* 2004;45:3662–3668.
44. Kelly DH. Visual response to time-dependent stimuli, I: amplitude sensitivity measurements. *J Opt Soc Am.* 1961;51:422–429.
45. Gebhard JW. Thresholds of the human eye for electric stimulation by different wave forms. *J Exp Psychol.* 1952;44:132–140.
46. Regan D. A high frequency mechanism which underlies visual evoked potentials. *Electroencephalogr Clin Neurophysiol.* 1968;25:231–237.
47. Tanino T, Kato S, Kawasumi M. Studies on electrically evoked pupillary reflex—indirect reflex and its frequency characteristic. *Jpn J Ophthalmol.* 1981;25:423–429.

Evaluating Neural Activity of Retinal Ganglion Cells by Flash-Evoked Intrinsic Signal Imaging in Macaque Retina

Gen Hanazono,[1,2,3] *Kazushige Tsunoda,*[1,2] *Yoko Kazato,*[1,2,4] *Kazuo Tsubota,*[5] *and Manabu Tanifuji*[2]

Purpose. Intrinsic signal imaging (ISI) detects light-induced microstructural or metabolic changes in retinal tissues. Thus, activities of the rod and cone systems could be mapped topographically. However, no direct evidence indicates the cellular origin of the signals. The purpose of this study was to determine whether and how retinal ganglion cells (RGCs) contribute to ISI.

Methods. In anesthetized macaque monkeys, the properties of intrinsic signals were investigated by simultaneous measurement of the retina and the primary visual cortex (V1) with different wavelengths of observation light, measurement of the flash-induced blood flow changes by laser Doppler flowmetry, and intravitreal injection of tetrodotoxin (TTX).

Results. Slow components of ISI correspond well to the flash-induced blood flow increase. Intrinsic signals of the posterior retina are partially decreased, and the signal of the optic disc is completely abolished by intravitreal injection of TTX at a concentration that should reduce the neural activities of RGCs. The intrinsic signal at the fovea did not change significantly after TTX injection.

Conclusions. Photoreceptors in the outer retina and RGCs in the inner retina are major contributors to the intrinsic signals, and the activity of the RGCs can be mapped by using fast and slow components of the signal in the posterior retina. The functional organization of the RGC layer has not been objectively mapped; results presented here indicate that the ISI has the potential to do this. (*Invest Ophthalmol Vis Sci.* 2008;49: 4655–4663) DOI:10.1167/iovs.08-1936

With the advancements in techniques, functional imaging of neural activities in the animal retina has become feasible by intrinsic signal imaging (ISI),[1–5] functional magnetic resonance imaging (fMRI),[6,7] and functional optical coherence tomography (fOCT).[8,9] Recently, the fast phototransduction process in single photoreceptor cells (flash-induced scintillation) in the living human eye could be observed with a high-speed flood-illumination retina camera equipped with adaptive optics.[10,11] These imaging techniques, though technically early for clinical application, may perhaps be used as diagnostic tools to detect various functional disorders in the human retina at the early stages, before subjective and anatomic disorders become permanent. For example, in the eyes of adults with glaucoma, one of the leading causes of blindness in the world,[12] the function of some retinal ganglion cells (RGCs) is altered, and the visual field is lost corresponding to the extent of the RGC dysfunction. However, it is well known that numerous RGCs have already lost their function before visual field loss can be detected by psychophysical examination.[13–15] Moreover, the activity of RGCs is not reflected in the conventional electrophysiological examinations, such as electroretinography (ERG). At present, there is no clinically established way to map objectively the dysfunctional area of RGCs over the retina. ISI is a well-established imaging technique recently used to translate neural activities elicited by photic or electrical pulses to visible changes in the appearance of the retina.[1–5] ISI has an advantage over fOCT and fMRI in that the response distribution of cone- and rod-induced retinal activities over the entire posterior ocular fundus can be topographically mapped with fine spatial resolution.[1,2] This is important because identification of the affected site is essential for the diagnosis and the treatment of diseases. The ISI, however, does not have spatial resolution in depth because it measures the light reflectance changes passing through all the retinal layers.

In our previous studies on the retina of macaque monkeys, we categorized the flash-induced intrinsic signals into fast and slow components: the fast signals peaked at 100 to 200 ms and were observed in the posterior retina including the fovea, and the slow signals peaked usually at more than 6 seconds and were observed at the optic disc and nonfoveal posterior retina.[1–5] Based on the response properties of the intrinsic signals together with the electroretinograms evoked by the same stimuli under different recording conditions, we propose that the slow components of retinal intrinsic signals reflect the activity of the inner or middle layer of the retina, though the cellular origin of this component has not been investigated in detail.

The purposes of this study were to investigate the source of each component of the intrinsic signals by simultaneous measurement of the ISI of the retina and the primary visual cortex (V1) with different wavelengths of observation light, to measure blood flow changes in the ocular fundus after a flash stimulus by laser Doppler flowmetry, and to measure ISI after intravitreal injection of tetrodotoxin citrate (TTX; Wako Pure Chemical Industries, Ltd., Osaka, Japan). Our results demonstrate that the time course of the intrinsic signal at the optic disc did not differ with the wavelength of the observation light, that the time course of the blood flow changes after a flash stimulus was approximately the same as the slow component of the intrinsic signals at the posterior retina and the optic disc.

From the [1]Laboratory of Visual Physiology, National Institute of Sensory Organs, Tokyo, Japan; [2]Laboratory for Integrative Neural Systems, Brain Science Institute, RIKEN, Saitama, Japan; [3]Department of Ophthalmology, Kikkoman General Hospital, Chiba, Japan; [4]Department of Ophthalmology, Nihon University School of Medicine, Tokyo, Japan; and [5]Department of Ophthalmology, Keio University School of Medicine, Tokyo, Japan.

Supported by Grant "Research on Sensory and Communicative Disorders" from the Ministry of Health, Labor and Welfare, Japan.

Submitted for publication February 26, 2008; revised April 15 and May 27, 2008; accepted August 13, 2008.

Disclosure: **G. Hanazono**, None; **K. Tsunoda**, None; **Y. Kazato**, None; **K. Tsubota**, None; **M. Tanifuji**, None

The publication costs of this article were defrayed in part by page charge payment. This article must therefore be marked "*advertisement*" in accordance with 18 U.S.C. §1734 solely to indicate this fact.

Corresponding author: Kazushige Tsunoda, Laboratory of Visual Physiology, National Institute of Sensory Organs, Tokyo Japan, 2-5-1 Higashigaoka, Meguroku, Tokyo 1528902, Japan; tsunodakazushige@kankakuki.go.jp.

and that TTX injection resulted in abolition of the slow component of the intrinsic signals at the posterior retina and the optic disc and in partial decrease of the fast component at the posterior retina though the signal at the fovea did not change. These results suggest that the slow components of the flash-induced intrinsic signals observed at the posterior retina and the optic disc reflect blood flow increases and that part of the fast component at the posterior retina reflected the local light-scattering changes. Both changes resulted, in part, from the activation of RGCs in the inner retina.

Methods

Experiments were performed on three rhesus monkeys (*Macaca mulatta*: M1, M2, M3) and one Japanese monkey (*Macaca fuscata*: M4). M1 was used for experiment 1, M2 and M3 were used for experiment 3, and M4 was used for experiment 2. The experimental protocol was approved by the Experimental Animal Committee of the RIKEN Institute, and all experimental procedures were carried out in accordance with the guidelines of the RIKEN Institute and the ARVO Statement for the Use of Animals in Ophthalmic and Vision Research.

After intramuscular injection of atropine sulfate (0.08 mg/kg), the monkeys were anesthetized with droperidol (0.25 mg/kg) and ketamine (5 mg/kg) and then were paralyzed with vecuronium bromide (0.1–0.2 mg/kg/h). They were artificially ventilated with a mixture of 70% N_2O, 30% O_2, and 1% to 1.5% isoflurane. Electroencephalograms, electrocardiograms, expired CO_2, and rectal temperatures were monitored continuously throughout the experiments. Before recordings, the pupils were fully dilated with topical tropicamide (0.5%) and phenylephrine hydrochloride (0.5%).

Three experiments were performed. In experiment 1, intrinsic signals were measured from the optic disc and primary visual cortex (V1) simultaneously with different wavelengths of the observation light to clarify the contribution of blood oxygenation. In experiment 2, flash-induced blood flow changes of the ocular fundus were measured by laser Doppler flowmetry and compared with the time course of the flash-induced intrinsic signals measured with an infrared observation light. In experiment 3, flash-induced intrinsic signals of the ocular fundus were measured before and after intravitreal injections of TTX. The effect of TTX was confirmed by measuring the photopic negative response (PhNR) of ERG.

Intrinsic Signal Imaging and Data Analyses

Procedures used to record the intrinsic signals have been described in detail.[1,2] A modified digital fundus camera system (NM-1000; Nidek, Aichi, Japan) was used to observe and measure light reflectance changes from the ocular fundus after 30 minutes of dark adaptation. The fundus was continuously monitored with light from a halogen lamp filtered through one of three band-pass interference filters: green (570 ± 10 nm), red (630 ± 20 nm), and infrared (870 ± 30 nm). For experiments 2 and 3, only the infrared filter was used. Fundus images were recorded with a CCD camera (PX-30BC; Primetech Engineering, Tokyo, Japan; spatial resolution, 640 × 480; temporal resolution, 1/30 seconds), and the images were digitized with a personal computer equipped with a video frame grabber board (Corona II; Matrox, Quebec, Canada; gray level resolution, 10 bits). The fundus camera photographed a 45° area of the posterior pole that included the fovea, superior and inferior vascular arcades, and optic disc.

Signal intensities were measured at three retinal sites: the fovea (15 × 15 pixels, 1.75° in diameter), the posterior retina between the fovea and the inferior temporal artery (95 × 25 pixels), and the optic disc (40 × 60 pixels). To compare the intensities of the intrinsic signals in experiment 3, we used the value of the lowest peak of the light reflectance of the foveal response (Fig. 4A, Fovea), the averaged value during the initial 500 ms after the flash for the fast component of the posterior retina (Fig. 4A, R_{fast}), and the averaged value during the last 500 ms at the end of recording trials for the optic disc response (Fig. 4A, Optic disc). To extract the slow component of the posterior retina, we subtracted the value R_{fast} from those during the last 1500 ms at the end of recording trials (Fig. 4A, R_{slow}).

To measure the flash-evoked intrinsic signals in the cortex (experiment 1), a stainless steel chamber (17 mm in diameter) was mounted on the skull over the contralateral side of V1 in M1. The skull and the dura mater were removed inside the chamber, and the chamber was filled with silicone oil (ADATO-SIL-OIL 1000; Bausch & Lomb GmbH, Heidelberg, Germany) and was tightly sealed with a glass coverslip to reduce the movement of the cortex. The cortical surface was illuminated by two fiber-optic light guides through the glass coverslip window, and light reflectance was recorded with the same type of a CCD camera used in retinal recording.[16,17] Light from a halogen lamp was filtered through three band-pass filters: green (570 nm), red (630 nm), and infrared (870 nm). The entire imaged area measured 8.8 × 6.6 mm and was imaged on 640 × 480 pixels. For the measurement of signal intensity, we averaged the light reflectance changes in the central region, which covered 3.05 × 3.63 mm (222 × 264 pixels; Fig. 1A, right). The camera was focused 500 μm below the cortical surface. A recording trial consisted of 300 (experiment 1), 360 (experiment 2), or 450 (experiment 3) video frames collected at a rate of 30 frames/s for a total recording time of 10, 12, or 15 seconds, respectively.

For stimulation, an unfiltered xenon flash (duration, 1 ms) was given to the entire posterior pole of the ocular fundus (500 ms in experiments 1 and 3 and 2 seconds in experiment 2 after the beginning of data acquisition). The flash luminance measured at the cornea was 56.1 cd · s/m^2, measured at 50.2 mm from the objective lens by a photoradiometer (IL1700; International Light Technologies, Peabody, MA). Timing of the data acquisition and stimulus delivery was under computer control.

Changes in light reflectance following stimulus—darkening [decrease in light reflectance] or brightening [increase in light reflectance]—of the retina were measured in the ocular fundus. Under infrared observation, the light reflectance of the entire posterior retina decreased (fundus image became darker) after flash stimulus. The optical signal was calculated as follows: grayscale values of the image obtained after the stimulus were divided, pixel by pixel, by those obtained during the prestimulus period, and this ratio was rescaled to 256 levels of grayscale resolution to show the stimulus-induced reflectance changes. To determine the time course of the flash-induced reflectance changes, the grayscale values of 15 video frames collected in 0.5 second were averaged for each datum point. We tried to make the total recording time as short as possible to keep the physiological conditions, such as corneal transparency, heart rate, and blood pressure, stable and to prevent photographic damage of the neural tissue

Figure 1. Intrinsic signals measured simultaneously from the optic disc and V1 with different wavelengths of the observation light. (**A**) Images of the recorded regions in experiment 1: ocular fundus (*left*) and cortical area V1 (*right*). Areas used for data analysis are shown by the *rectangles*. (**B**) Time courses of two-dimensional images of the ocular fundus (*left*) and cortical area V1 (*right*) showing the light reflectance changes evoked by a flash stimulus recorded with different wavelengths of the observation light. Thirty consecutive video frames collected during 1 second were averaged for one poststimulus image. Darkened regions indicate a decrease of light reflectance after the flash stimulus. Note that foveal regions observed with 570 and 630 nm become brighter after the flash because of the strong bleaching of cone photopigments. (**C**) Plot of the time courses of flash-evoked light reflectance changes. The time after the flash is shown on the abscissa, and the delivery of the flash is indicated by the *arrowhead* (same in the following figures). Each point is the average of 15 video frames collected during 0.5 second of the light reflectance changes. Averages of 10 trials are shown with the SE of the means. (**D**) Plot of the time courses of flash-evoked light reflectance changes, presented as relative values to the maximum in the optic disc and V1

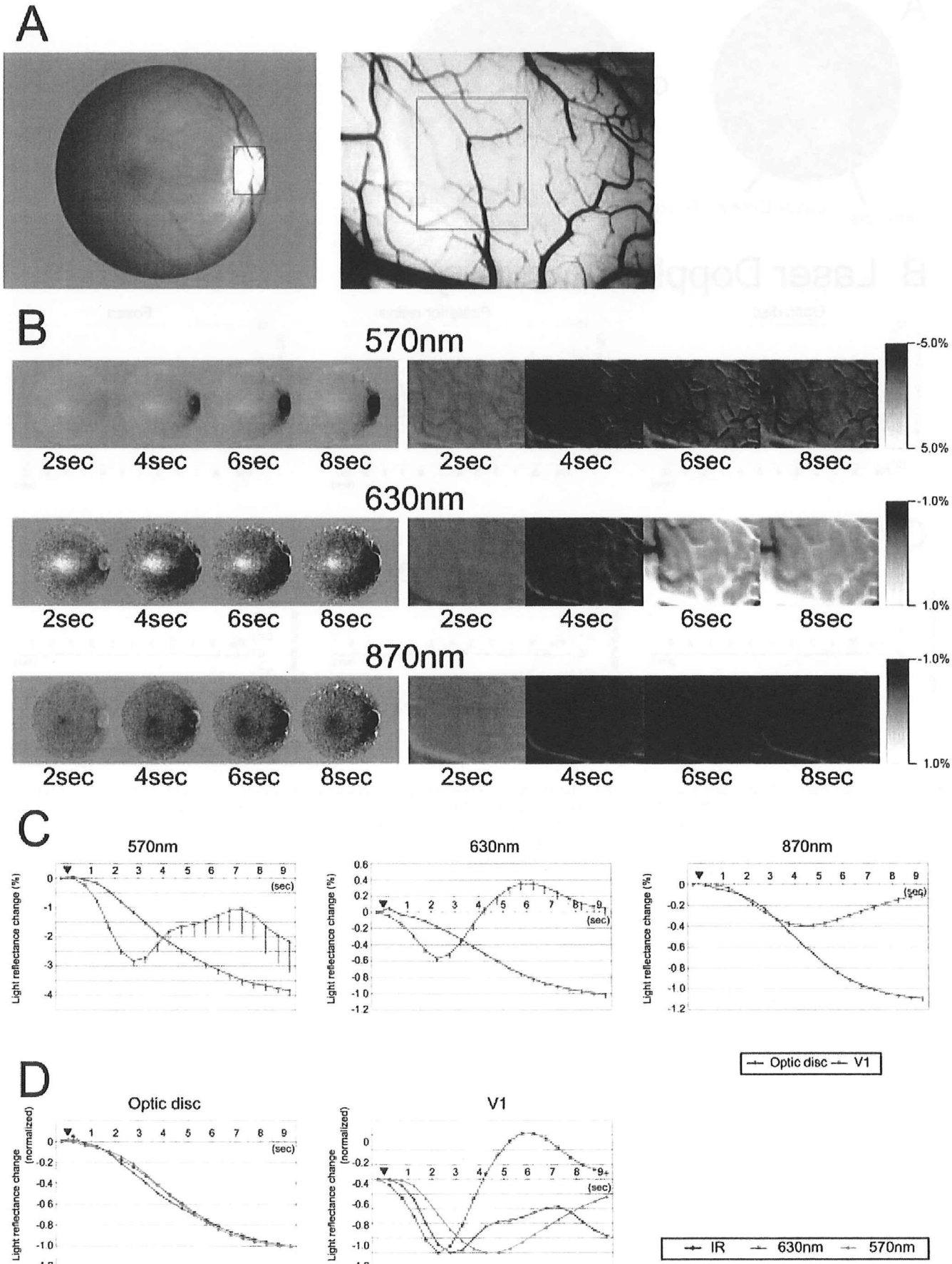
A
B
570nm
2sec
4sec
6sec
8sec
-5.0%
5.0%
630nm
-1.0%
1.0%
870nm
C
570nm
630nm
870nm
Light reflectance change (%)
(sec)
Optic disc
V1
D
Optic disc
V1
Light reflectance change (normalized)
IR
630nm
570nm

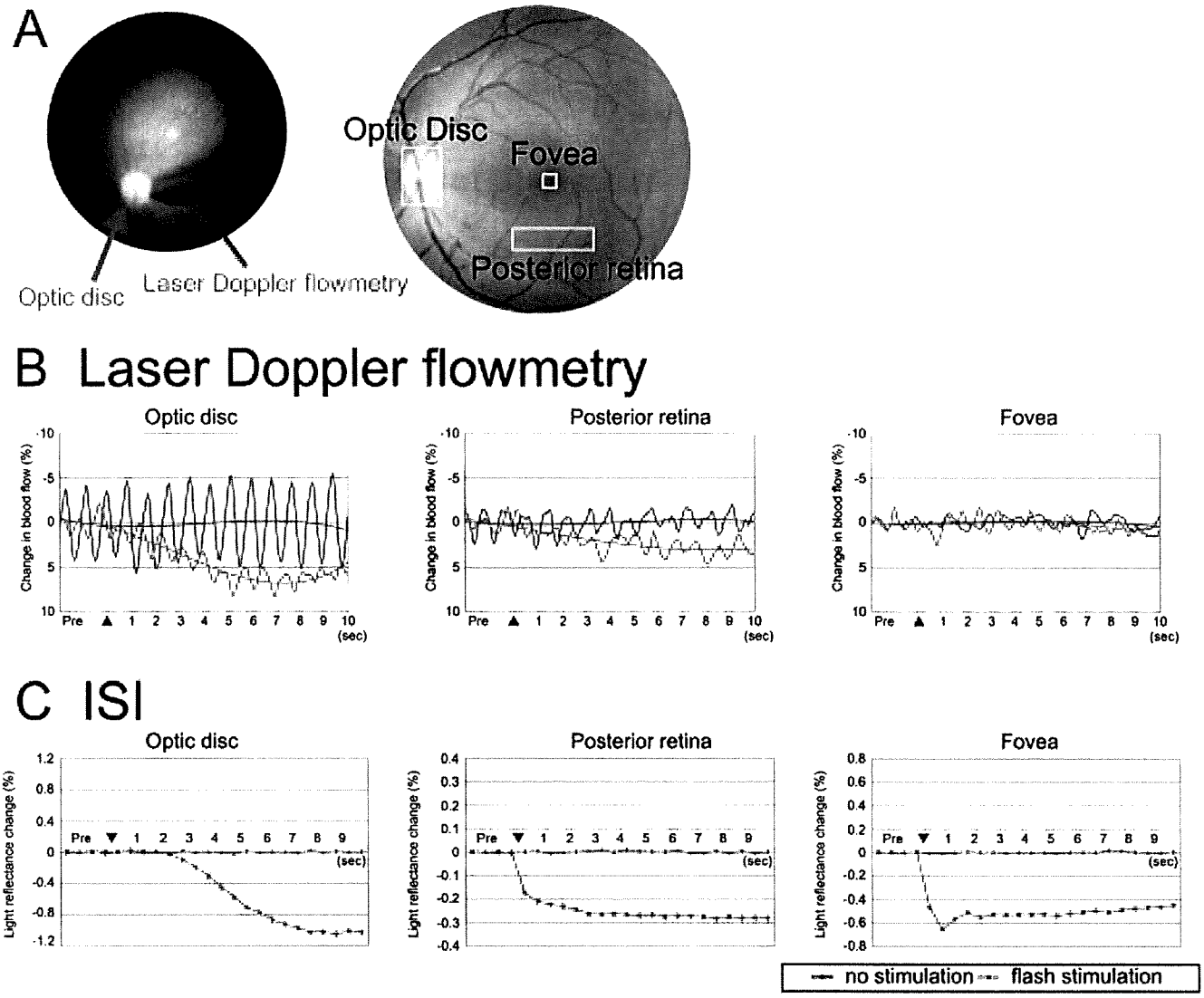

FIGURE 2. Flash-induced blood flow changes of the ocular fundus by a laser Doppler flowmetry. (A, *left*) Measurement of blood flow at the optic disc by laser Doppler flowmetry. The probe in the vitreous cavity and the location of the optic disc are indicated by arrows. *Right*: fundus photograph of normal retina showing the regions for the ISI analysis in experiment 2. (B) Plot of the time courses of blood flow changes with (*red*) or without (*blue*) flashes, measured with a laser Doppler flowmetry, from three locations indicated in (A). Averages of 20 trials are shown with polynomial trendlines (order 3). (C) Plot of the time courses of light reflectance changes with (*red*) or without (*blue*) flashes measured by the ISI, from three locations indicated in (A). Averages of 10 trials are shown with SE.

by the visible observation light. The data of 10, 10, and 15 consecutive trials were averaged in experiments 1, 2, and 3, respectively.

Measuring Blood Flow by Laser Doppler Flowmetry (Experiment 2)

Flash-induced blood flow changes were measured in the left eye of M4 by a laser Doppler flowmetry system (Periflux 5010; Perimed, Stockholm, Sweden; solid-state diode laser, 780 μm; power, <1 mW; probe, PF403; probe diameter, 450 μm; fiber separation, 250 μm; time constant, 0.03 s) under aseptic conditions. After local peritomy of the conjunctiva, the laser probe was inserted through a scleral port made at the 2 o'clock position 3 mm from the corneal limbus. The size of the sclerotomy was small enough to keep the intraocular pressure normal and constant during recording. The laser probe was fixed firmly by a manual micromanipulator placed in front of the monkey's face. For measurement of the blood flow changes at the optic disc and the perimacular region, the tip of the probe was placed less than 1 mm above the target (Fig. 2A) and was directed on the vessel-free regions to measure the averaged blood flow changes in capillaries. Blood flow was represented in arbitrary units (perfusion unit [PU]). Blood flow changes evoked by the same intensity of flash stimulus was calculated by dividing blood flow after the stimulus by the averaged blood flow during a 2-second period before the stimulus. Data of 20 consecutive trials were averaged.

TTX Injection (Experiment 3)

TTX dissolved in physiological saline (50 μL, 8 μM), was injected into the vitreous cavity of the left eye of M2 and M3 under anesthesia. Before injection, 50 μL aqueous humor was removed from the corneal limbus by a 27-gauge needle. TTX was then injected though the pars plana (3 mm posterior to the corneal limbus) into the geometric center of the vitreous by a 27-gauge needle at the superior temporal position. The same amount of saline was injected by the same procedure into the vitreous cavity of the fellow eye for control recordings. Slow intrinsic signals of the optic disc and the posterior retina are very sensitive,[2] and if small local regions in which RGC function has not been completely blocked remain, the blood flow increase of the optic disc may be strongly triggered for that local region. Thus, we had to

completely block RGC responses over the entire retina. Moreover, the intrinsic signals were susceptible to the physiological conditions, such as intraocular pressure, corneal curvature, and vitreous transparency, of the whole body and of the eyeball. To obtain sufficient pharmacologic blockade and recovery of the physiological condition of the eye, the recording was not conducted on the day of injection. Intrinsic signal imaging and electroretinographic recordings were made 1 week before TTX injection, 1 day after injection, and 4 weeks after injection.

Electroretinographic Recordings (Experiment 3)

Electroreginograms were recorded under light-adapted conditions on the same day of the ISI measurements. An LED contact lens electrode with a background illumination source (Mayo, Aichi, Japan) was inserted into one of the eyes. After 15 minutes of light adaptation (background, 25 cd/m^2), a white flash of intensity 3 cd · s/m^2, duration 3 ms, was given 15 times at 1-second intervals. Electroretinograms were amplified 10,000× and the band-pass filters were set at 0.3 to 500 Hz (PowerLab; AD Instruments, Colorado Springs, CO). The PhNR was measured from the baseline to the first negative trough after b-wave in the single-flash cone ERG (Fig. 3A).[18,19]

Results

Experiment 1

The time course of the intrinsic signals evoked by three wavelengths (570, 630, and 870 nm) of the observation light were compared at the optic disc and cortical area V1 (Fig. 1). Although the absolute reflectance changes were different (Fig. 1C), the time course of the changes at the optic disc was the same for the three wavelengths (Fig. 1D). Reflectance slowly decreased after the flash and reached its negative peak at the end of the recording period.[2] The time course at cortical area V1, on the other hand, differed for the different wavelengths (Figs. 1C, 1D). The onset of reflectance decrease was the earliest with 630 nm, followed by 570 nm and 870 nm. With 630 nm, the light reflectance change reached a negative peak 2 seconds after flash and was followed by an increase in the light reflectance that overshot the baseline reflectance. With 540 nm and 870 nm, the light reflectance change reached a negative peak at 3 and 4.5 seconds after flash, respectively, but the large overshoot increase was not observed. This pattern in the time course of the signals in cortical area V1 was the same as when a grating stimulus was used.[16,20]

Experiment 2

Flash-induced blood flow changes of the ocular fundus were measured by laser Doppler flowmetry and were compared with the intrinsic signals evoked by the same flash intensity. The retina was observed by infrared light (Fig. 2). Blood flow at the optic disc gradually increased after the flash and reached a peak 7.5 seconds after the flash (Fig. 2B). This time course was similar to that of the intrinsic signals (Fig. 2C). Similarly, the blood flow in the posterior retina gradually increased after the flash and reached a peak at 8 seconds (Fig. 2B). This time course, however, was different from that of the intrinsic signal. The time course of the blood flow at the posterior retina did not have the fast changes observed in the ISI (Fig. 2C).

We have reported[2] that the flash-evoked intrinsic signal in the posterior retina had two components, a fast light-reflectance decrease that peaked at 100 to 200 ms (Fig. 4A, R_{fast}) and a slow light-reflectance decrease that peaked at 6 seconds or later (Fig. 4A, R_{slow}).[2] Blood flow changes in the posterior retina seemed to match only the slow component of the ISI. In the foveal area, a flash-evoked blood flow change could not be observed by laser Doppler flowmetry, though large and fast light reflectance decreases were observed in the ISI (Figs. 2B, 2C).

Experiment 3

Flash-induced intrinsic signals of the ocular fundus were measured before and after intravitreal injection of TTX (Fig. 3). On the day of each recording, photopic electroretinograms were recorded to evaluate inner retinal activity by measuring the PhNR.[18,19] From all the components of the electroretinogram, only the PhNR amplitude was reduced after TTX injection, and it recovered to normal levels 4 weeks after injection (Fig. 3A).

Pseudocolor maps of the signal distribution, averaging 7 to 9 seconds after flash, in the posterior pole are shown in Figure 3A. One day after TTX injection, intrinsic signals at the optic disc and the posterior retina, but not the foveal region, were reduced. The signal at the fovea did not change. Four weeks after injection, responses in the whole posterior pole appeared to be the same as before injection.

The time course of the intrinsic signals before and after TTX injection is shown in Figure 3B. The response at the optic disc was abolished after TTX injection. The fast component was partially reduced at the posterior retina, and the slow component was completely abolished by TTX injection. The response at the fovea was not affected by TTX injection.

Amplitudes of the four components of the intrinsic signals (optic disc, R_{fast}, R_{slow}, Fovea) for 3 recording days in two monkeys were compared (Fig. 4). Statistical analyses was performed with the Mann–Whitney U test to compare group means, and the differences were considered significant when $P < 0.05$. No significant changes were observed in the control eyes either in the optic disc or in the posterior retina. Signals of the optic disc and the R_{slow} component were abolished 1 day after TTX injection. R_{fast} signals were significantly reduced 1 day after injection (59.9% and 78% compared with preinjection levels in M2 and M3, respectively). The intensity of the foveal response was not changed by TTX injection, but statistical analysis could not be used for the foveal responses because the foveal response required 30 minutes of dark adaptation, and only the initial trial after adaptation could be used for the comparison.[2]

Discussion

Experiment 1

We have measured the flash-evoked intrinsic signals simultaneously from the optic disc and cortical area V1. The three wavelengths, 570 nm, 630 nm, and 870 nm, of the observation light were selected because they could best determine the changes in blood volume, deoxygenated hemoglobin, and tissue light scattering, respectively. We found that the time course of the intrinsic signals in area V1 had a typical pattern, similar to that recorded with grating stimulus by other authors.[16,20] The reflectance pattern at the optic disc was the same at all wavelengths (Fig. 1D), suggesting that the slow signal observed at the optic disc was not related to the degree of oxygenation of the hemoglobin.

It is generally assumed that light-scattering changes represent microscopic morphologic changes elicited by neural activity, such as cell swelling associated with ion and water movements and changes in synaptic vesicle density associated with synaptic transmission. Light-scattering changes are believed to be free of changes in blood flow and oxygenation, and amplitudes are constant whichever wavelength is used as the observation light.[16]

The amplitude of the signal at the optic disc, however, was almost four times larger at 570 nm than at 630 nm or 870 nm.

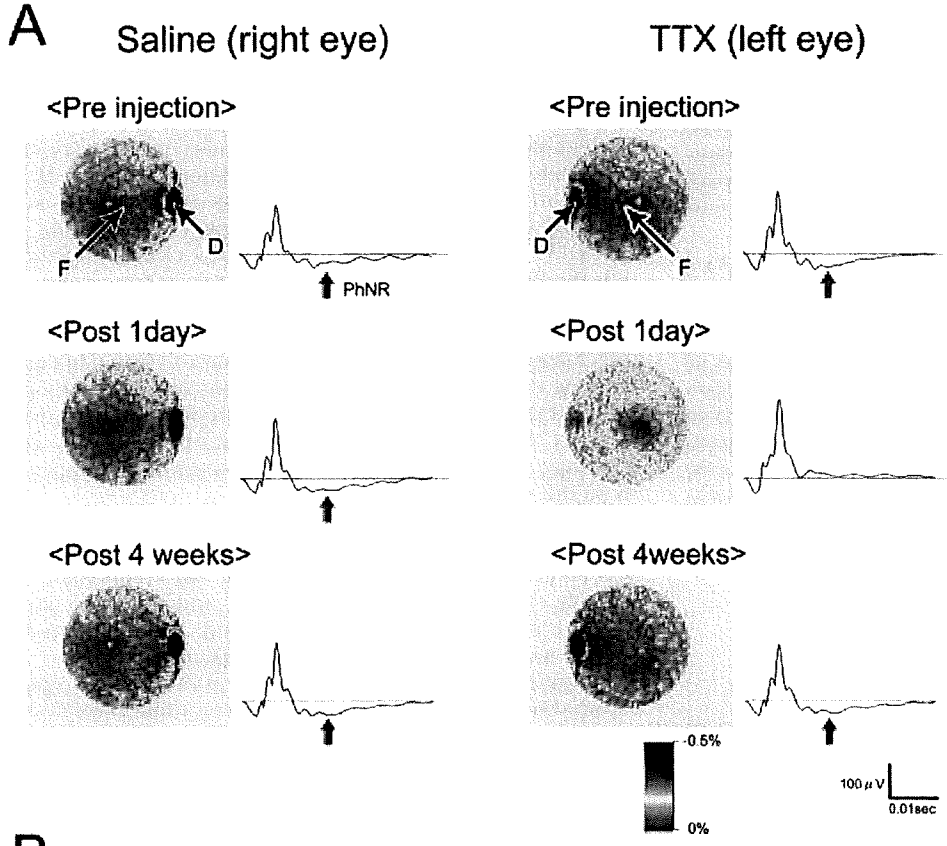

FIGURE 3. Intrinsic signals of the ocular fundus before and after the intravitreous injection of TTX. (**A**) Pseudocolor response topography of flash-evoked light reflectance changes with saline or TTX injection, measured before, 1 day after, and 4 weeks after injection. Each image was the average from 7 to 9 seconds after a flash. Electroretinographic responses recorded on the same day. *Arrows*: locations of optic disc (D) and fovea (F). *Red arrows*: PhNR. (**B**) Plot of the time courses of light reflectance changes with saline or TTX injection, measured from three locations indicated in Figure 2A. Results before, 1 day after, and 4 weeks after injection are shown by different colors. In the optic disc and posterior retina, the averages of 15 trials are shown with SE.

probably because the increase of the light-scattering signal at the optic disc reflected changes in the flow of red blood cells in the vessels, which were triggered by the neural activity in the inner retina. It is well known that hemoglobin absorbs more green light than red light. The ratio of blood-related light reflectance changes to the total tissue light reflectance changes can be larger when illuminated at 570 nm than at 630 nm or 870 nm; this was confirmed by the results of experiment 2.

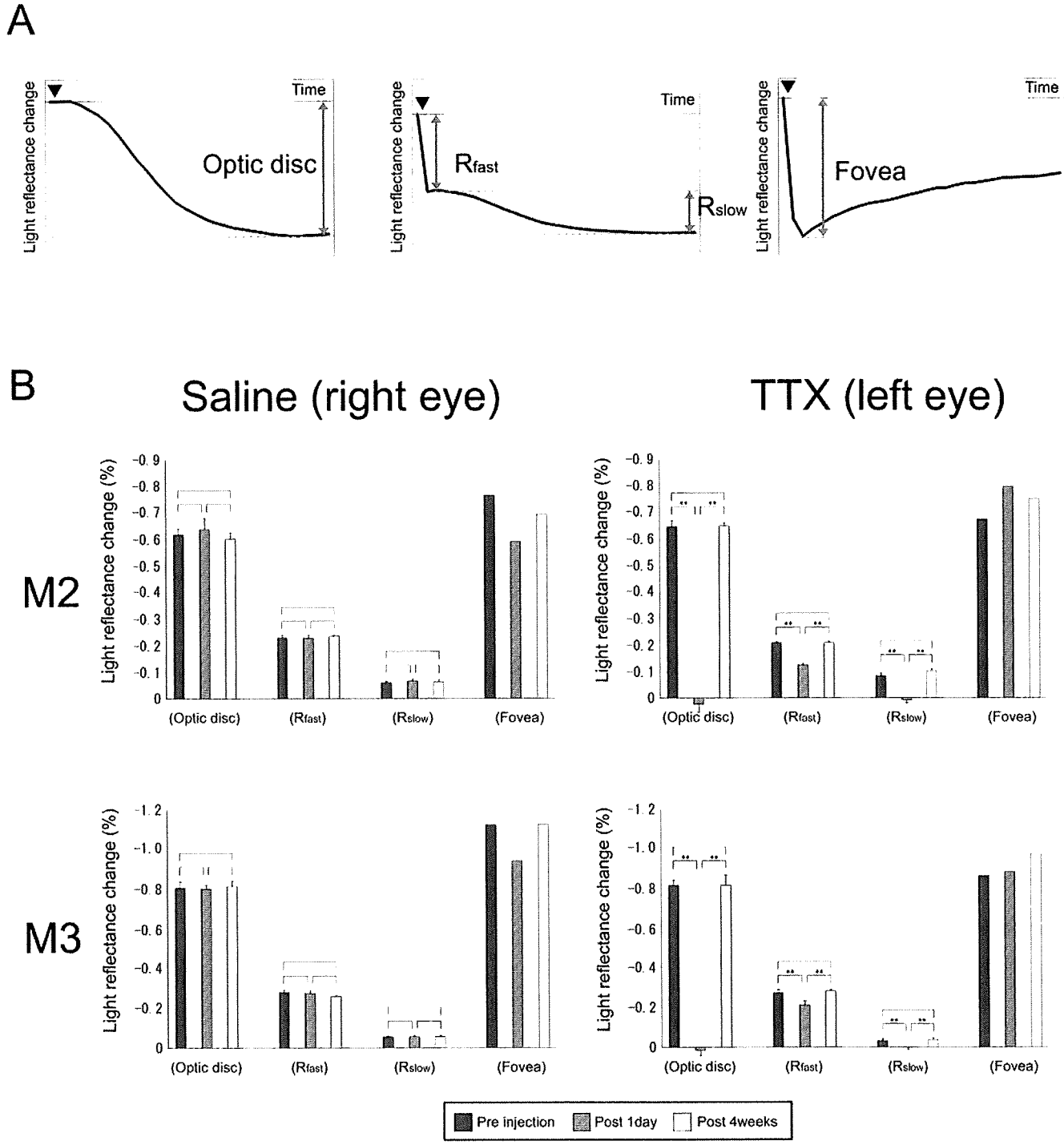

FIGURE 4. Change in four components of intrinsic signals after TTX injection. (A) Definition of the four components in flash-evoked intrinsic signals. (B) Changes in ISI signals after saline or TTX injection are shown for four signal components in M2 and M3. $^{**}P < 0.01$, statistically significant.

Experiment 2

Experiment 2 showed that the slow intrinsic signals at the optic disc and the posterior retina reflected blood flow increases after stimulation. The fast changes observed in the ISI at the fovea and the posterior retina could not be detected by a laser Doppler flowmetry. Although the fast intrinsic signals were relatively large, they were independent of blood flow changes. At the fovea, the blood flow changes are believed to reflect changes in the choroidal blood flow because of the absence of capillaries in the central 300 μm of the retina. Blood flow in this region was constant even after a flash stimulus.

Riva et al.[21,22] showed that blood flow on the optic nerve head measured by laser Doppler flowmetry increased after diffuse flicker stimulation in cats and humans.[21,22] The stimulus duration used in their studies was as long as 60 seconds, and the precise time course of the signals immediately after stimulus onset could not be determined. However, with extensive experiments, together with the data of patients with glau-

coma, they concluded that flash-evoked blood flow changes were induced by the activity of the RGCs.[21–24]

Experiment 3

The RCGs are the major retinal elements in retina that have spiking activity, and TTX can reduce the activity of RCGs by blocking the Na^+-dependent spikes.[25,26] The PhNR is known to be reduced in eyes with experimental glaucoma and after TTX injection and, thus, is highly dependent on the spiking activity of inner retinal neurons.[18,19] In our study, one of the eyes was injected with TTX, and the inner retinal activity was completely blocked. This suggested that the slow intrinsic signals observed at the posterior retina and the optic disc represented the blood flow increase after flash-induced spiking activity in the inner retina. Foveal signal was not affected by TTX at all because there are no RGCs in the foveal region.

Part of the fast component of the posterior retina represents the spiking activity of the inner retina and is attributed to light-scattering changes but is not related to blood flow. Another part of the fast intrinsic signals at the posterior retina that was not affected by TTX might have originated from activity from more distal neurons than the RGCs. The cellular origin of the non–blood-related fast light-scattering signals, however, may not be easily solved because each type of neural cells (photoreceptors, bipolar cells, Müller cells) may have its own independent characteristics for producing reflectance changes after neural activation. Recently, in vivo fOCT showed that the properties of the flash-evoked light-scattering changes were different in the outer and inner segments of the photoreceptors.[8,9]

Amacrine cells are also known to produce spikes, and the proportion of amacrine cells that contribute to the intrinsic signal is unknown. We should remember that the slow intrinsic signals in the posterior retina and the optic disc do not represent the activity of RCGs exclusively. Riva et al.[24] have shown that the blood flow increases at the optic disc after flickering flash stimulus is abnormally reduced in patients with ocular hypertension and early glaucoma. Considering that RGCs but not amacrine cells are the major neural elements affected by these disorders,[13–15,27–29] it is reasonable that the reduction of RGC activity in the posterior pole can be detected by the ISI.

Conclusions

Recently, a selective reduction in the PhNR of the electroretinogram has been reported in patients with glaucoma and optic nerve diseases.[18,19] Although the PhNR had been expected to be used to detect glaucoma at its early stage, it must be remembered that the electroretinogram is the mass response of the whole retina and that no spatial information, such as the location of scotoma in the Bjerrum area, can be obtained by this technique. Some attempts have been made to map the RGC function objectively by multifocal ERG.[30–32] However, it is still impossible to precisely discriminate the dysfunctional region of RGCs because of low spatial resolution.

The ISI, on the other hand, has high spatial resolution and is limited mainly by the resolution of the CCD camera and biological artifacts produced by the subjects. Our results showed that fast and slow signal components in the posterior retina were reduced by TTX. Theoretically, the fast signal component should have better spatial resolution because it is produced directly by the light-scattering changes immediately after neural activation of the inner retina. The slow signal, on the other hand, may not have such a good spatial resolution because it reflects the blood flow increases after neuronal activities, and the mechanisms underlying neurovascular coupling in the primate retina are still under investigation.

It is believed that stimulus-induced blood flow changes can be regulated by chemical mediators, such as nitrogen oxide, pH, and pCO_2,[33,34] but it is still unknown how close neural activity and blood flow increases correspond. Peppiatt et al. have recently reported that pericytes in the retinal capillaries can modulate the blood flow in response to changes in neural activity in isolated rat retinas. They proposed that a mechanism exists that finely regulates local blood flow at the capillary level.[35] If this is correct, then stimulus-evoked blood flow change may be used as a probe by which the activated region of the retina can be precisely mapped. This indicates that not only the fast but also the slow signals in the posterior retina may be used to map the functional status of the RGCs. Although correspondence between a region of low visual sensitivity and a reduction of the ISI signals should be confirmed in experimental animal models or in patients with local visual field defects, the ISI has the potential to be a diagnostic tool for mapping the functional status of the RGCs topographically.

References

1. Tsunoda K, Oguchi Y, Hanazono G, Tanifuji M. Mapping cone- and rod-induced retinal responsiveness in macaque retina by optical imaging. *Invest Ophthalmol Vis Sci* 2004;45:3820–3826.
2. Hanazono G, Tsunoda K, Shinoda K, Tsubota K, Miyake Y, Tanifuji M. Intrinsic signal imaging in macaque retina reveals different types of flash-induced light reflectance changes of different origins. *Invest Ophthalmol Vis Sci.* 2007;48:2903–2912.
3. Inomata K, Tsunoda K, Hanazono G, et al. Distribution of retinal responses evoked by trans-scleral electrical stimulation detected by intrinsic signal imaging in macaque monkeys. *Invest Ophthalmol Vis Sci.* 2008;49:2193–2200.
4. Abramoff MD, Kwon YH, Ts'o D, et al. Visual stimulus-induced changes in human near-infrared fundus reflectance. *Invest Ophthalmol Vis Sci.* 2006;47:715–721.
5. Okawa Y, Fujikado T, Miyoshi T, et al. Optical imaging to evaluate retinal activation by electrical currents using suprachoroidal-transretinal stimulation. *Invest Ophthalmol Vis Sci.* 2007;48:4777–4784.
6. Duong TQ, Ngan SC, Ugurbil K, Kim SG. Functional magnetic resonance imaging of the retina. *Invest Ophthalmol Vis Sci.* 2002;43:1176–1181.
7. Cheng H, Nair G, Walker TA, et al. Structural and functional MRI reveals multiple retinal layers. *Proc Natl Acad Sci U S A.* 2006;103:17525–17530.
8. Bizheva K, Pflug R, Hermann B, et al. Optophysiology: depth-resolved probing of retinal physiology with functional ultrahigh-resolution optical coherence tomography. *Proc Natl Acad Sci U S A.* 2006;103:5066–5071.
9. Srinivasan VJ, Wojtkowski M, Fujimoto JG, Duker JS. In vivo measurement of retinal physiology with high-speed ultrahigh-resolution optical coherence tomography. *Opt Lett.* 2006;31:2308–2310.
10. Jonnal S, Rha J, Zhang Y, Cense B, Gao W, Miller D. In vivo functional imaging of human cone photoreceptors. *Optics Express.* 2007;15:16141–16159.
11. Zhang Y, Cense B, Rha J, et al. High-speed volumetric imaging of cone photoreceptors with adaptive optics spectral domain optical coherence tomography. *Optics Express.* 2006;14:4380–4394.
12. Quigley HA. Number of people with glaucoma worldwide. *Br J Ophthalmol.* 1996;80:389–393.
13. Quigley HA, Green WR. The histology of human glaucoma cupping and optic nerve damage: clinicopathologic correlation in 21 eyes. *Ophthalmology.* 1979;86:1803–1830.
14. Quigley HA, Addicks EM, Green WR. Optic nerve damage in human glaucoma, III: quantitative correlation of nerve fiber loss and visual field defect in glaucoma, ischemic neuropathy, papilledema, and toxic neuropathy. *Arch Ophthalmol.* 1982;100:135–146.
15. Quigley HA, Dunkelberger GR, Green WR. Retinal ganglion cell atrophy correlated with automated perimetry in human eyes with glaucoma. *Am J Ophthalmol.* 1989;107:453–464.

16. Bonhoeffer T, Grinvald A. Optical imaging based on intrinsic signals: the methodology. In: Toga AW, Mazziotta JC, eds. *Brain Mapping*. San Diego: Academic Press; 1996:55–97.
17. Tsunoda K, Yamane Y, Nishizaki M, Tanifuji M. Complex objects are represented in macaque inferotemporal cortex by the combination of feature columns. *Nat Neurosci*. 2001;4:832–838.
18. Viswanathan S, Frishman LJ, Robson JG, Harwerth RS, Smith EL 3rd. The photopic negative response of the macaque electroretinogram: reduction by experimental glaucoma. *Invest Ophthalmol Vis Sci*. 1999;40:1124–1136.
19. Viswanathan S, Frishman LJ, Robson JG, Walters JW. The photopic negative response of the flash electroretinogram in primary open angle glaucoma. *Invest Ophthalmol Vis Sci*. 2001;42:514–522.
20. Fukuda M, Rajagopalan UM, Homma R, Matsumoto M, Nishizaki M, Tanifuji M. Localization of activity-dependent changes in blood volume to submillimeter-scale functional domains in cat visual cortex. *Cereb Cortex*. 2005;15:823–833.
21. Riva CE, Harino S, Shonat RD, Petrig BL. Flicker evoked increase in optic nerve head blood flow in anesthetized cats. *Neurosci Lett*. 1991;128:291–296.
22. Riva CE, Logean E, Falsini B. Temporal dynamics and magnitude of the blood flow response at the optic disk in normal subjects during functional retinal flicker-stimulation. *Neurosci Lett*. 2004;356:75–78.
23. Riva CE, Falsini B, Logean E. Flicker-evoked responses of human optic nerve head blood flow: luminance versus chromatic modulation. *Invest Ophthalmol Vis Sci*. 2001;42:756–762.
24. Riva CE, Salgarello T, Logean E, Colotto A, Galan EM, Falsini B. Flicker-evoked response measured at the optic disc rim is reduced in ocular hypertension and early glaucoma. *Invest Ophthalmol Vis Sci*. 2004;45:3662–3668.
25. Narahashi T. Chemicals as tools in the study of excitable membranes. *Physiol Rev*. 1974;54:813–889.
26. Bloomfield SA. Effect of spike blockade on the receptive-field size of amacrine and ganglion cells in the rabbit retina. *J Neurophysiol*. 1996;75:1878–1893.
27. Glovinsky Y, Quigley HA, Dunkelberger GR. Retinal ganglion cell loss is size dependent in experimental glaucoma. *Invest Ophthalmol Vis Sci*. 1991;32:484–491.
28. Frishman LJ, Shen FF, Du L, et al. The scotopic electroretinogram of macaque after retinal ganglion cell loss from experimental glaucoma. *Invest Ophthalmol Vis Sci*. 1996;37:125–141.
29. Kerrigan-Baumrind LA, Quigley HA, Pease ME, Kerrigan DF, Mitchell RS. Number of ganglion cells in glaucoma eyes compared with threshold visual field tests in the same persons. *Invest Ophthalmol Vis Sci*. 2000;41:741–748.
30. Sutter EE, Bearse MA Jr. The optic nerve head component of the human ERG. *Vision Res*. 1999;39:419–436.
31. Hood DC, Bearse MA Jr, Sutter EE, Viswanathan S, Frishman LJ. The optic nerve head component of the monkey's (*Macaca mulatta*) multifocal electroretinogram (mERg). *Vision Res*. 2001;41:2029–2041.
32. Kurtenbach A, Leo-Kottler B, Zrenner E. Inner retinal contributions to the multifocal electroretinogram: patients with Leber's hereditary optic neuropathy (LHON): multifocal ERG in patients with LHON. *Doc Ophthalmol*. 2004;108:231–240.
33. Buerk DG, Riva CE, Cranstoun SD. Nitric oxide has a vasodilatory role in cat optic nerve head during flicker stimuli. *Microvasc Res*. 1996;52:13–26.
34. Kondo M, Wang L, Bill A. The role of nitric oxide in hyperaemic response to flicker in the retina and optic nerve in cats. *Acta Ophthalmol Scand*. 1997;75:232–235.
35. Peppiatt CM, Howarth C, Mobbs P, Attwell D. Bidirectional control of CNS capillary diameter by pericytes. *Nature*. 2006;443:700–704.

網膜の機能的イメージング

角田 和繁

IRYO Vol. 62 No. 7 (404－406) 2008

要旨 眼底の画像診断技術は近年めざましい進歩をとげており，なかでも網膜微細構造の観察を可能にする光干渉断層計：Optical Coherence Tomography (OCT) は，網膜疾患の診断，治療に関する従来の常識を一変させるほど臨床応用価値の高いものであった．一方で，網膜の神経機能を客観的に評価する検査法はいまのところ網膜電図 (ERG) に限られており，網膜の神経機能をイメージングすることは眼底画像解析の究極の目標ともいえるものである．本稿では，新しい網膜機能検査法である網膜内因性信号計測法：Functional Retinography (FRG) について紹介する．

キーワード：網膜内因性信号計測法，機能的イメージング，光学計測法

FRGとは

著者らは網膜の神経機能を客観的に評価する目的で大脳皮質における機能的マッピングの手法である光学計測法(Optical Imaging)を眼底に応用し，FRGという網膜機能のイメージング法を世界に先駆けて開発した[1)-3)]．

神経活動にともなって神経組織の微細構造が変化すると，そこから戻ってくる光の強さ（光反射率）はその活動の強さに応じて変化する．FRGとはフラッシュ刺激に対する網膜の神経活動を，光の反射率変化を利用して2次元的にマッピングする技術である．信号の発生起源として，網膜外層の光散乱変化（視反応にともなう細胞の体積変化など），および網膜内層の血流増加などが考えられている．

まだ開発途上にある技術であるが，将来の臨床応用に向けて大きな可能性をもった，機能的眼底画像解析法である．

測定方法

サルを用いた動物実験においては，全身麻酔で眼球運動を停止させ，眼底カメラを改良した観察系を用いて眼底をCCDカメラでモニターする（図1A）．眼底観察には近赤外光（870nm）を用いる．測定開始から0.5秒後に眼底後極部を白色キセノンフラッシュ（1ms）にて刺激し，観察光の網膜反射率を刺激前後で比較する．刺激後に画像の明るさが変化している部分が神経活動のおきた領域に相当し，通常は神経活動の高い領域が反射率低下のために暗くみえる（図1B）．

国立病院機構東京医療センター　臨床研究センター視覚生理学研究室
別刷請求先：角田和繁　東京医療センター　臨床研究センター視覚生理学研究室
〒152-8902　東京都目黒区東が丘2－5－1
（平成20年5月28日受付）
Serises of Articles on Sensory Disorders 7
Functional Imaging of the Retina
Kazushige Tsunoda
Key Words: functional retinography, functional imaging, optical imaging

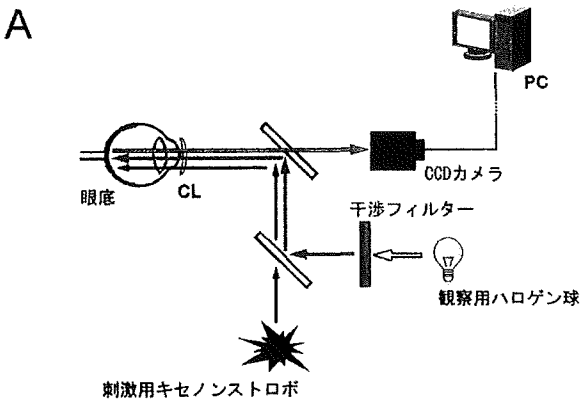

図1　A：FRGシステムの概要　B：びまん性白色フラッシュ刺激によるFRG信号の時間経過

FRGで何がわかるか

1．視細胞の神経活動分布[1)]

白色フラッシュ刺激によって視細胞が活動すると，網膜全体の反射率が早期に低下し早い内因性信号が観察される（ピーク：150msec）．これは網膜外層の光散乱変化を反映している．信号強度を3Dで表示すると，明順応下では中心窩に信号のピークを認め，周辺部に向かって減少するが（図2A），暗順応下では中心窩に加えて周辺部にドーナツ状のピークを認める（図2B）．内因性信号のピークは中心窩では錐体視細胞，周辺部では杆体視細胞の解剖学的な分布に一致している．

2．網膜内層，視神経乳頭上の血流変化[2)]

レーザードップラー血流計を用いた研究により，光刺激によって網膜中心動脈の血流が一過性に増加することが知られている．フラッシュ刺激によって生じる内因性信号のうち遅い反応は網膜内層の神経活動による血流増加を反映しており，眼底後極部，および視神経乳頭で観察される（ピーク：5-10sec）．図3は刺激後に視神経乳頭の血流が増加する様子を示しており，とくに中心動静脈の部位で高いピークがみられる．

3．網膜局所刺激によるFRG信号[2)]

網膜に局所フラッシュ刺激を行うと，刺激部位に相当する網膜に限局した内因性信号を記録することができる（図4）．これはFRGの空間解像度の高さを示している．

4．FRGとERGの比較[2)]

同一の刺激に対するFRGとERGの信号を比較すると，暗順応状態では，中心窩を除く網膜面の遅い反応と視神経乳頭部の反応の閾値が，ERG-b波の閾値とほぼ一致している．これはFRGがERGと同程度に鋭敏な感度を持つ検査法であることを示している．なお，覚醒下のヒトでも局所フラッシュ刺激により網膜内因性信号は測定可能であるが，現在のところ，詳細なマッピングを行うことはまだ困難である．

まとめ

FRGの利点として，非侵襲的であること，空間分解能が高いこと，測定時間が短いことなどがあげられる．問題点としては，ヒトの測定時に生じる固

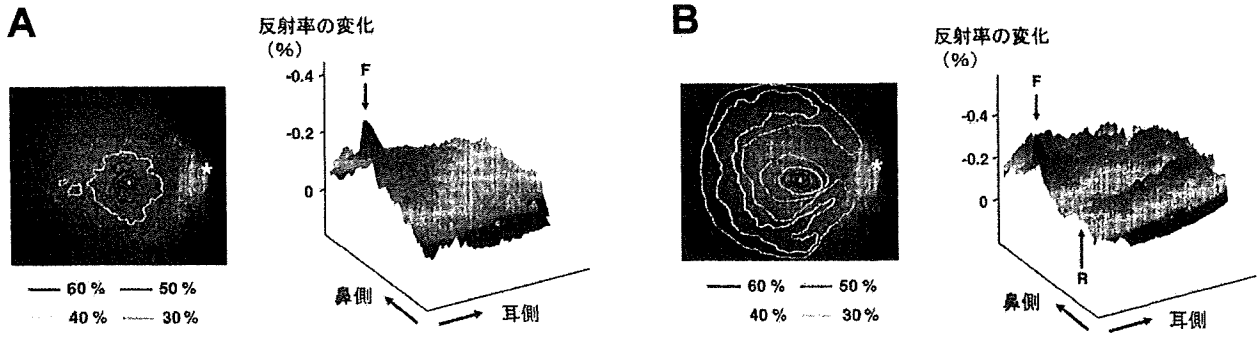

図2　びまん性白色フラッシュ刺激によるFRG信号分布
（A：明順応下，B：暗順応下．それぞれ右に下半網膜の3次元トポグラフィーを示す）．Fは中心窩，Rはrod ring.

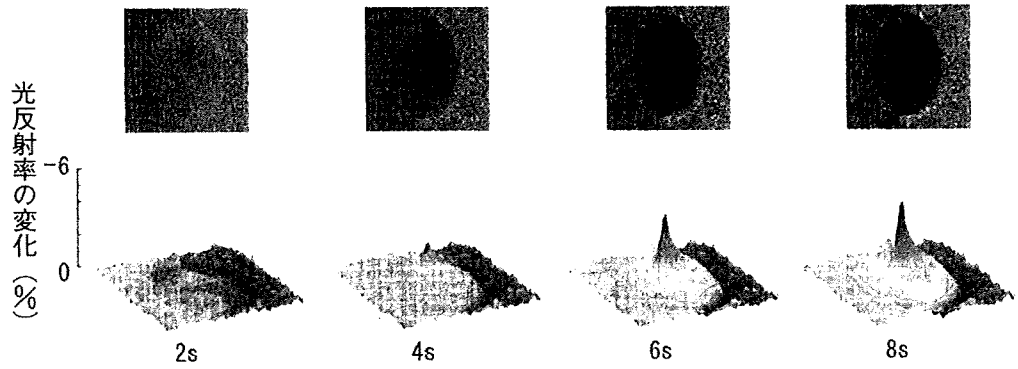

図3　視神経乳頭部におけるFRG信号のトポグラフィー

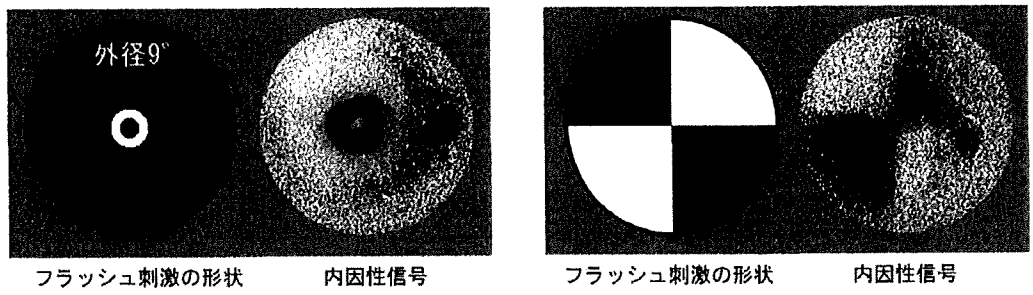

図4　局所網膜刺激によるFRG信号のトポグラフィー
左のシェーマで白く描かれた部位が刺激領域を示す．

視微動等により，画質が著しく低下することであり，現在それを克服すべく研究を行っている．将来臨床応用が可能になれば黄斑変性症や網膜色素変性症などさまざまな網膜疾患において精度の高い他覚的機能評価が可能になると期待されている．

さらにFRG以外の機能的眼底画像解析法として，OCTを利用して神経機能評価を行う研究が注目されている．これは2002年に理化学研究所のMaheswariらによって初めて提唱されたFunctional OCT[4]という概念を網膜に応用したものであり，臨床応用に向けた研究がわれわれのグループをはじめとしてさかんに行われている[5]．網膜の神経機能をイメージングするという研究は新しい診断法として高く注目されており，将来は新たな網膜機能評価法として確立される日が来ることが期待される．

[文献]

1）Tsunoda K, Oguchi Y, Hanazono G et al. Mapping Cone-and Rod-Induced Retinal Responsiveness in Macaque Retina by Optical Imaging. Invest Ophthalmol Vis Sci 2004；45：3820-6.

2）Hanazono G, Tsunoda K, Shinoda K et al. Intrinsic Signal Imaging in Macaque Retina Reveals Different Types of Flash-induced Light Reflectance Changes of Different Origins. Invest Ophthalmol Vis Sci 2007；48：2903-12.

3）Inomata K, Tsunoda K, Hanazono G et al. Distribution of Retinal Responses Evoked by Transscleral Electrical Stimulation Detected by Intrinsic Signal Imaging in Macaque Monkeys. Invest Ophthalmol Vis Sci 2008；49(5)：2193-200.

4）Maheswari RU, H. Takaoka, R. Homma et al. Implementation of optical coherence tomography (OCT) in visualization of functional structures of cat visual cortex. Opt Commun 2002；202：47-54.

5）Srinivasan VJ, Wojtkowski M, Fujimoto JG et al. In vivo measurement of retinal physiology with high-speed ultrahigh-resolution optical coherence tomography. Opt Lett 2006；31：2308-10.

機能的 OCT は可能か

角田　和繁*

機能的イメージングとは

今日の眼科臨床において，視機能の評価は視力，視野，色覚，中心フリッカ値など主に患者の自覚的検査によってなされている。これらによって示される結果は眼球から大脳視覚中枢までの機能を統合した視機能であり，実際の診断のためには網膜，視神経，大脳皮質など，さらに個々の器官の機能を評価していく必要がある。その評価のために重要なのは，患者の応答によらない他覚的（客観的）な検査法であり，網膜では網膜電図（ERG）がこれに相当する。

一方，眼科における画像診断技術（イメージング）は近年めざましい進歩をとげてきた。例えば光干渉断層計（optical coherence tomograph：OCT）は，検眼鏡によって捉えることのできない網膜微細構造の観察を可能にするものであり，特に現在主流となりつつあるフーリエドメイン OCT を用いると網膜各層を短時間かつ高解像度で評価できる。しかし，OCT によって計測されるのはあくまでも解剖学的構造であり，これによって視細胞をはじめとする網膜の神経活動を捉えることはできない。

機能的イメージング（functional imaging）とは，上述の客観的機能評価とイメージング技術とを組み合わせたものであり，神経機能の空間的分布を地図（トポグラフィ）のようにわかりやすく示すのが目的である。

例えば functional MRI は，視覚刺激などによって神経活動の増強した部位を血液中酸素飽和度を反映する信号（BOLD signal）によって特定し，通常の MRI 画像に重ね合わせることによって，脳内活動部位の地図を提示する技術である。

OCT から functional OCT へ（構造解析から機能解析へ）

OCT はレーザー光の干渉現象を利用して組織の断面構造を描出する技術であり，網膜のみならず角膜，隅角，あるいは心血管など他の組織においても応用されている。これに対して理化学研究所の Maheswari ら[1,2]は，OCT 信号を用いて神経機能のリアルタイムの計測が可能であることを 2002 年にネコの大脳皮質を用いて示し，functional OCT という新しい概念を提唱した。

では，なぜ OCT を用いて神経活動を捉えることができるのだろうか。

神経活動に伴って神経組織の微細構造や光反射率が変化する現象は古くから知られており[3,4]，光を使って生体脳の神経活動を測定する光学計測法（optical imaging）が 1990 年頃からさかんに行われてきた[5,6]。網膜の断層構造においても，光刺激に伴う光異性化反応，それに伴う膜電位の変化，細胞周囲のイオン環境の変化などによってレーザーの反射強度が変化しているはずである。この変化

* つのだ・かずしげ　国立病院機構東京医療センター臨床研究センター，理化学研究所脳科学総合研究センター
別刷請求先：角田和繁　〒152-8902　目黒区東が丘 2-5-1　国立病院機構東京医療センター臨床研究センター

0370-5579/08/￥500/論文/JCLS

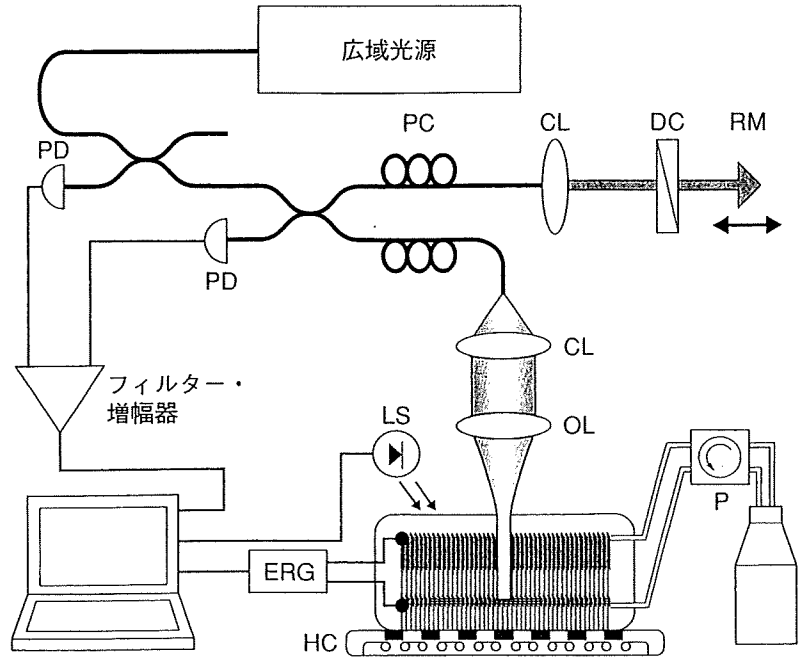

図1　Drexler らの functional OCT システム
灌流液(P)で保存した摘出網膜に光刺激(LS)を与え，OCT（上方）と網膜電図（ERG）で計測する。
CL：光軸補正レンズ，P：灌流装置，HC：温熱チェンバー，OL：対物レンズ，PC：偏波コントローラー，DC：分散補正装置，RM：参照鏡，PD：フォトダイオード。(文献[11]より改変して転載)

を OCT 信号の変化として捉えて神経活動マップとして描出するのが functional OCT であり，網膜においても，大脳皮質と同様に光刺激前後の信号強度を比較することで，刺激によって惹起された“evoked response”を抽出することができる。

なお，同様の原理を眼底画像上に二次元的に応用した技術が網膜内因性信号計測法であり，フラッシュ刺激前後の眼底画像を比較することで，神経活動に伴う網膜の光散乱変化をマッピングしている[7~10]。これについては別項で花園が詳しく解説している（「網膜内因性信号計測装置」の項参照）。

Functional OCT の目ざすもの

では，functional OCT が実用化されると，われわれ眼科医にとってどのようなメリットがあるのだろうか。

網膜は大まかには視細胞を中心とした外層（脈絡膜からの酸素供給），および神経節細胞を中心とした内層（網膜血管からの酸素供給）に分けられる。さらに，視細胞，双極細胞，神経節細胞，水平細胞，アマクリン細胞などといった，神経生理学的に役割の異なる各種の神経細胞が層状に分布している。眼底疾患は，神経線維層から視細胞，網膜色素上皮，さらには脈絡膜まで，病気の種類によって異常の起きている部位はさまざまである。

Functional OCT では網膜機能の異常を層別に識別することができるため，網膜機能不全の原因がどの層にあるかということを，リアルタイムで示すことができる。例えば黄斑円孔や糖尿病黄斑浮腫，加齢黄斑変性症などで，黄斑部のどの層が，どの範囲で機能的に傷害されているのかを具体的に図示し，それを経時的に比較して診断に役立てることができる。オカルト黄斑症や AZOOR (acute zonal occult outer retinopathy) のように，通常眼底に異常のみられない疾患ではさらにその意義が大きい。また，さまざまな遺伝性ジストロフィや先天性停止性夜盲などにおいては，その傷害部位が網膜中層にあるのか，外層にあるのかなど，疾患の起源を明らかにすることができるかもしれない。

これまでに行われた網膜の functional OCT 研究

これまでに論文発表されたデータで代表的なものは，Drexler らによるタイムドメイン OCT を用いた摘出網膜（ウサギ）の実験[11]と，Fujimoto ら